

NPS ARCHIVE  
1960  
FARREN, M.

800740

①  
570

ADAPTIVE SAMPLING FREQUENCY FOR  
SAMPLED-DATA CONTROL SYSTEMS

MERRITT C. FARREN  
and  
CHARLES A. PHILLIPS

Loan Copy

POSTI	WHITE SECTION <input type="checkbox"/>
REG	DIFF SECTION <input checked="" type="checkbox"/>
UNANNOUNCED	<input type="checkbox"/>
<i>Per form 50</i> <i>PT</i>	
BY	DATE/TIME/AVAILABILITY *
EXT.	MAN. NO. OF SPEC. L.
<i>2</i>	

*U.S.*

*✓ Cool. 035*

**Library**  
 U. S. Naval Postgraduate School  
 Monterey, California









ADAPTIVE SAMPLING FREQUENCY  
FOR  
SAMPLED-DATA CONTROL SYSTEMS

\* \* \* \* \*

Merritt C. Farren  
and  
Charles A. Phillips



A 107









ADAPTIVE SAMPLING FREQUENCY  
FOR  
SAMPLED-DATA CONTROL SYSTEMS

by  
Merritt C. Farren  
and  
Charles A. Phillips

This work is accepted as fulfilling  
the thesis requirements for the degree of  
MASTER OF SCIENCE  
IN  
ELECTRICAL ENGINEERING  
from the  
United States Naval Postgraduate School

---



## ABSTRACT

Sampled-data control systems generally have fixed sampling frequencies which must be set high enough to give satisfactory performance for all anticipated conditions. A study is made here of an adaptive system which varies the sampling frequency by measuring a system parameter. It is shown that a sampler followed by a zero-order hold whose sampling period is controlled by the absolute value of the first derivative of the error signal will be a more "efficient" sampler than a fixed frequency sampler. That is, over a given time interval, fewer samples are needed with the variable frequency system than with a fixed frequency system while maintaining essentially the same response characteristics.

Analog computer studies of simple type 1 and type 2 sampled-data servo systems with error sampling and unity feedback verified the method. Standard analog computer components were used to set up a simulated servo system, a rate detector, absolute value detector, a voltage controlled oscillator, and a sampler and zero-order hold.

The system described reduced the number of samples required for response to a step input to about three-quarters that required in a fixed sampling frequency system. Over a long period of time, savings in the number of samples required can be expected to be between twenty-five and fifty per cent. In many applications, the saving produced by reducing the overall number of samples required may outweigh the added complexity of the adaptive sampling frequency system.



## ACKNOWLEDGMENTS

The authors wish to express their appreciation for the assistance given them by the engineers and technicians of the Servomechanisms Section of the Philco Corporation, Western Development Laboratories, Palo Alto, California, where this study was begun, and in particular to Mr. Lynn J. Harvey, Mr. Eddie Wong, and Dr. Gene F. Franklin of Stanford University, a Philco Consultant. The authors also wish to express their appreciation to Professor Richard A. Dorf, Department of Electrical Engineering, U. S. Naval Postgraduate School, Monterey, California, for his guidance and suggestions.





## TABLE OF CONTENTS

Chapter	Title	Page
I	Introduction	1
II	The Basic Sampled-Data Control System	4
III	Variable Frequency Sampling	15
IV	Servo System with Variable Sampling Frequency	23
V	Adaptability	35
VI	Conclusions and Recommendations	40
References		43
Bibliography		44
Appendices		
A	Complete Analog Computer Simulation	45
B	Sampler and Zero-Order Hold Simulator	51
C	Differentiator and Absolute Value Detector	63
D	The Voltage Controlled Oscillator	72
E	Transistorized Relay Control	85
F	Root Locus Analysis in the Z-Plane	88



CHAPTER I  
INTRODUCTION

This thesis presents the investigation of a sampled-data feedback control system employing an adaptive, variable frequency sampler. The basic area of investigation was concerned with finding a system signal and the functions of that signal for controlling the variable frequency sampler so that the sampling would be more efficient. Sampling is defined to be more efficient when similar output response characteristics are obtained with fewer samples. The investigation was limited to the extent that only readily available system signals or signals which could be generated in a simple manner from some system signal were considered as controlling signals for the variable frequency sampler.

The problem was attacked with the aid of analog computer studies. All of the necessary system component circuits were simulated on the analog computer. The entire system was composed of a simple servo, a variable frequency sampler and zero order hold circuit, a differentiating circuit, an absolute value detection circuit, a voltage controlled, variable frequency oscillator and a transistorized relay control circuit. Type I and type II servo systems were investigated and it was found that the number of samples necessary for specified output response characteristics could be substantially reduced using aperiodic sampling. A method of sampling frequency control using a function of the first derivative of the error signal was developed. It was found that the sampling frequency, in the



interest of efficiency could be increased as necessary, toward an upper bound during the transient state and decreased toward a lower bound during steady state conditions.

The thesis topic was suggested at the Philco Corporation, Western Development Laboratories, as an investigation that might produce profitable results. It was desired that some method of variable frequency sampling control be found which would reduce the total number of samples required while maintaining the same response characteristics. The purpose of the reduction of the number of samples required was to extend the lifetime of digital shaft encoders and also to enhance the possibilities of computer time sharing.

A survey of the literature indicated that this sampling problem had not yet been investigated. Many studies have been recently made concerning sampled data feedback control systems with periodic sampling.<sup>1,2,3,4</sup> Direct applications of the periodic sampling principle are, however, relatively limited. A more difficult and more promising problem is that of aperiodic sampling control.<sup>5</sup> Methods have been developed for analyzing aperiodic sampling systems as an aid toward understanding and synthesizing these non-linear systems. However, the problem of designing or implementing the aperiodic sampling control, has not been investigated. The authors could find no published or unpublished literature treating the problem of aperiodic sampling as applied to total sample reduction without response characteristic degradation.

The following chapters will discuss the basic sampled-data



control systems, the control of variable frequency aperiodic sampling, the results of the analog computer studies and the system adaptive qualities with respect to aperiodic sampling. It is hoped that this thesis will help to extend the explored area in the realm of sampled-data servomechanisms.





## CHAPTER II

### THE BASIC SAMPLED-DATA CONTROL SYSTEM

One basic sampled-data feedback control system was chosen for study. The block diagram of the system is shown in Fig. 1.

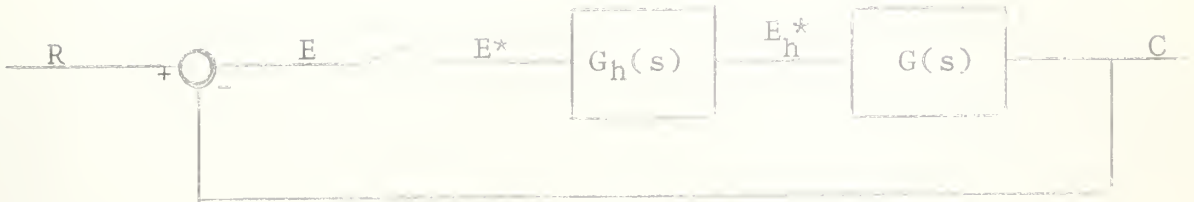


Figure 1. Basic sampled-data control system.

The basic sampled-data control system was investigated using two different transfer functions  $G(s)$ . This chapter will consider the basic sampled-data control system with fixed period sampling only. The desired minimum and maximum fixed frequency sampling periods will be discussed. The discussion is separated into two sections; the first section describes the type II servo system and the second section describes the type I servo system.

The transfer function  $G(s) = \frac{K(s + a)}{s^2}$  produces a type II servo system.  $G_h(s)$  is a zero order hold. The z-plane root-locus analysis is discussed in Appendix F. It is seen that the z-plane transfer function of this type II sampled-data system is:

$$G(z) = \frac{K_1(z + z_1)}{(z - 1)^2}$$

where

$$K_1 = KT\left(1 + \frac{aT}{2}\right)$$

$$z_1 = \frac{aT - 2}{aT + 2}$$



The maximum period  $T$  was determined by the steady state stability requirements. Two conditions determine the region of stable response of the closed loop system. These simultaneous conditions are:

$$0 < aT \leq 2$$

and

$$0 < KT \leq 2$$

Therefore, with both  $a$  and  $K$  given as fixed values, the range of  $T$  for stable closed loop response is determined by:

$$0 < T \leq \frac{2}{a} \quad \text{for } a > K$$

and

$$0 < T \leq \frac{2}{K} \quad \text{for } a < K$$

Fig. 2(c) illustrates a reasonable sampling period  $T$  for steady state stability conditions. The Brush recording of Fig. 2(c) shows the system response with system parameters  $K = 15$ ,  $a = 10$ , and  $T = .096$ . Since  $a < K$ , the maximum period  $T$  for system stability is determined by  $T = 2/K = .133$ . Thus it is seen that  $T = .096$  is near the limit of  $T$  for stable response and the peak overshoot is nearly 100%.

The minimum sampling period  $T$  was determined by the largest value of  $T$  that produced a response similar to that of a continuous system. Fig. 3 illustrates this range of sampling periods for a system with  $a = 10$  and  $K = 10$ . In Fig. 3 it is seen that the system response is practically the same when  $T = .016$  or  $T = .025$ . For comparison, Table 1 contains the pertinent values from Fig. 3. The table shows that with respect to output response characteristics very little is gained by sampling faster than  $T = .043$ . With system



parameters  $a = 10$  and  $K = 15$ . Fig. 2(a) shows that  $T = 0.044$  is also a reasonable lower limit for this system, and Fig. 2(b) demonstrates that increasing  $T$  to 0.053 sec. increases the peak overshoot and settling time only slightly.

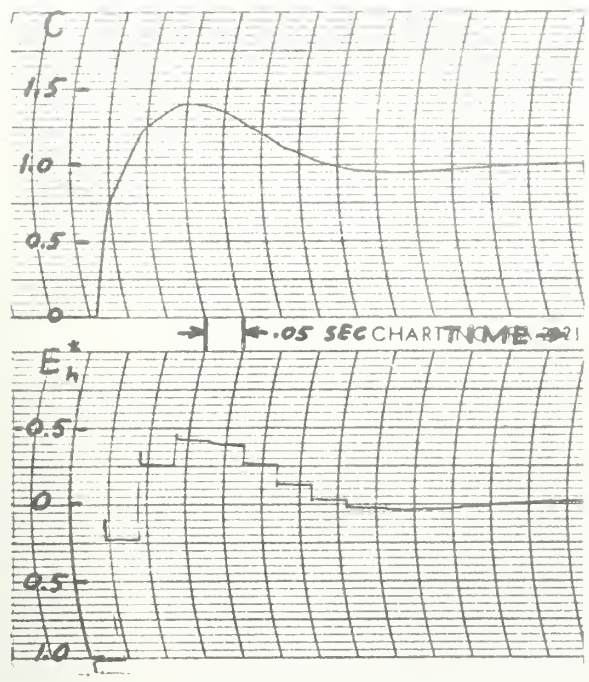
T (Seconds)	Rise Time	Peak Overshoot	Time of Peak Overshoot	5% Settling Time
.016	.125	40%	.30	.813
.025	.125	40%	.30	.813
.043	.115	45%	.28	1.075
.080	.075	60%	.25	1.150

Table 1. Comparison of fast sampling responses.

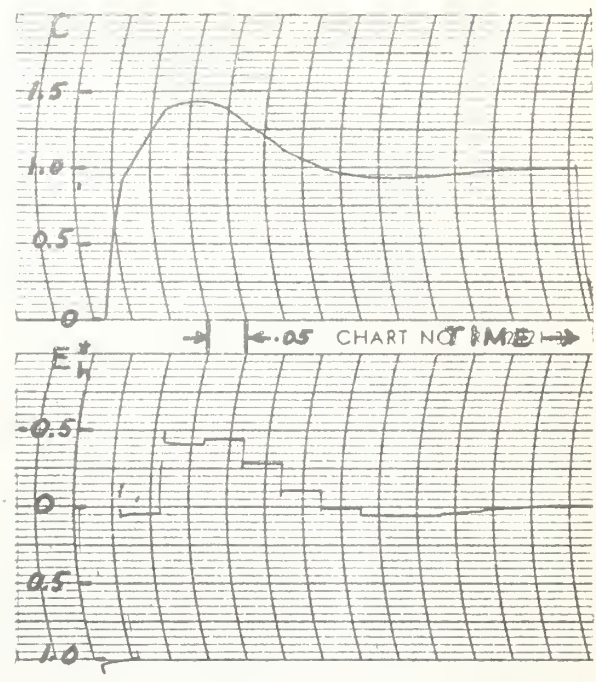
Fig. 4 illustrates the accuracy with which the analog computer simulated system represents the theoretical mathematical model with respect to stability criterion. In both examples of Fig. 4,  $a > K$  so the maximum  $T$  for a stable response is determined by the relation  $T = 2/a = .100$ . The theoretical response of the closed loop system at  $T = .100$  is a stable, undamped periodic response. Fig. 4(a) shows the steady state response where  $a = 20$ ,  $K = 7.5$ , and  $T = .1006$ . Fig. 4(b) shows the steady state response where  $a = 20$ ,  $K = 15$ , and  $T = .1006$ . Both figures illustrate that the various simulated components are accurate representations of the system mathematical model.

The type I servo is produced by the transfer function  $G(s) = \frac{K}{s(s + b)}$ . The z-plane root-locus is discussed in

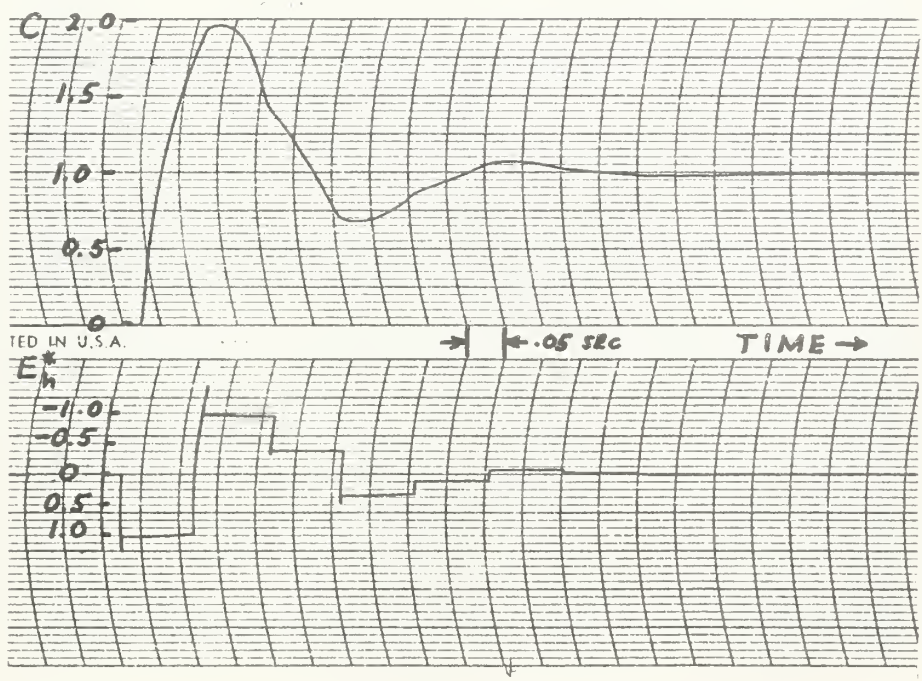




(a)  $T = 0.044$



(b)  $T = 0.053$



(c)  $T = 0.096$

Fig. 2. Fixed rate responses for type II system where  $K = 15$  and  $a = 10$ . Suitable range of  $T$  represented by  $.044 \leq T \leq .096$ . The graphs are recordings of the closed loop system response and the output of the zero order hold to a unit step input.





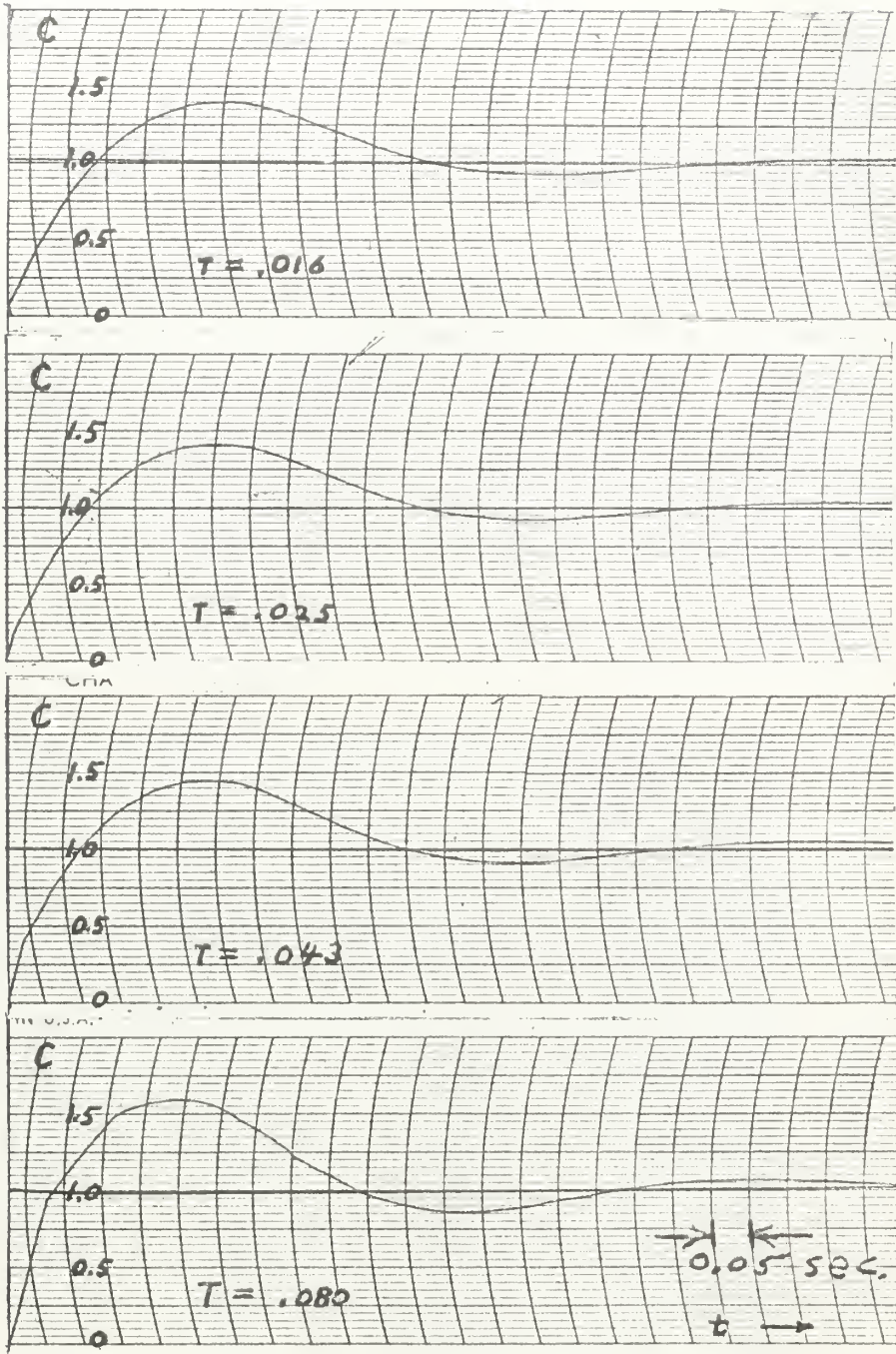
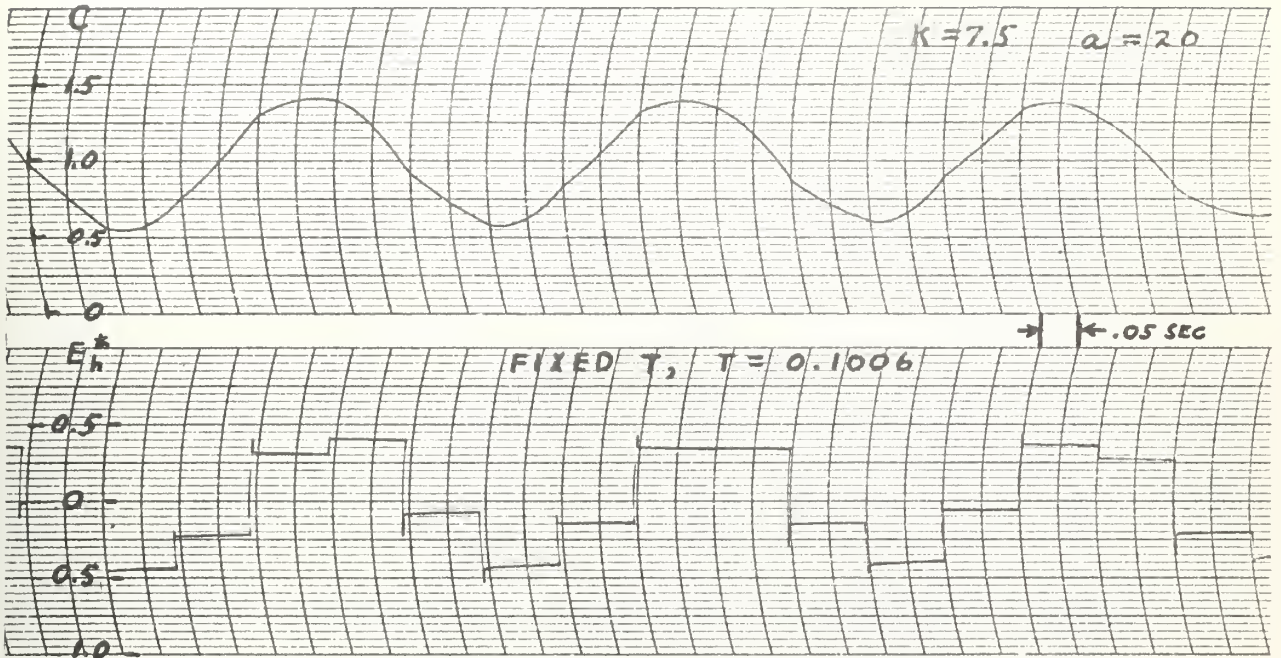
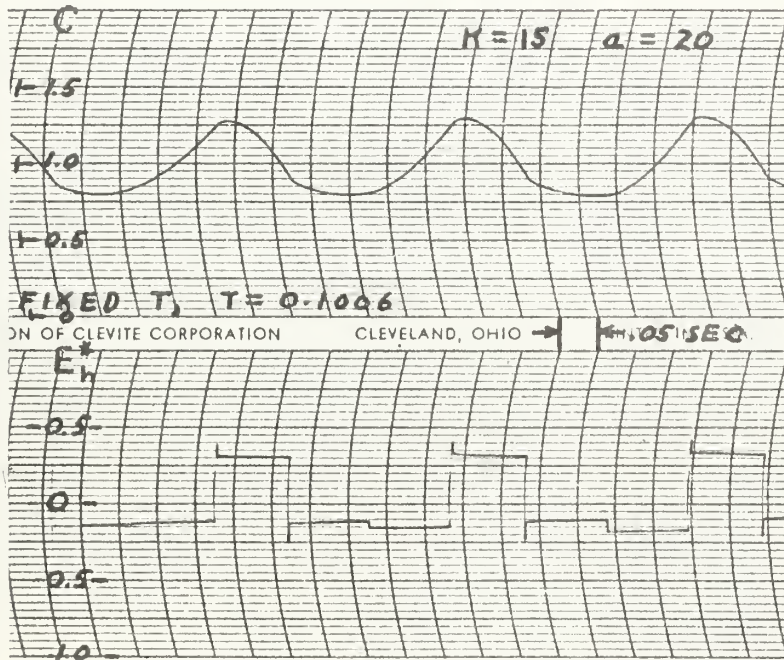


Fig. 3. Determining the minimum sampling period  $T$ . For practical purposes the system response to a unit step input is essentially the same for all  $T \leq .043$ . Therefore it is unnecessary to sample faster than  $T = .043$  seconds.





(a) Steady state response at limit of stability.



(b) Steady state response at limit of stability.

Fig. 4. Brush recordings illustrating closeness of analog computer results to the theoretically determined results. The theoretical steady state response at  $T=0.10$  is a stable, undamped periodic oscillation.



Appendix F. It is seen that the z-plane transfer function is:

$$G(z) = \frac{K_1(z + z_1)}{(z - p_1)(z - 1)}$$

$$K_1 = \frac{K}{b^2}(bT + e^{-bT} - 1)$$

$$z_1 = \frac{1 - e^{-bT}(1 + bT)}{bT + e^{-bT} - 1}$$

$$p_1 = e^{-bT}$$

From Table F-1 in Appendix F, it is seen that if  $bT > 3.71$ , then the relationship between T and K for the stable response region is:

$$0 < K \leq \frac{2b^2(1 + e^{-bT})}{bT(1 + e^{-bT}) - 2(1 - e^{-bT})},$$

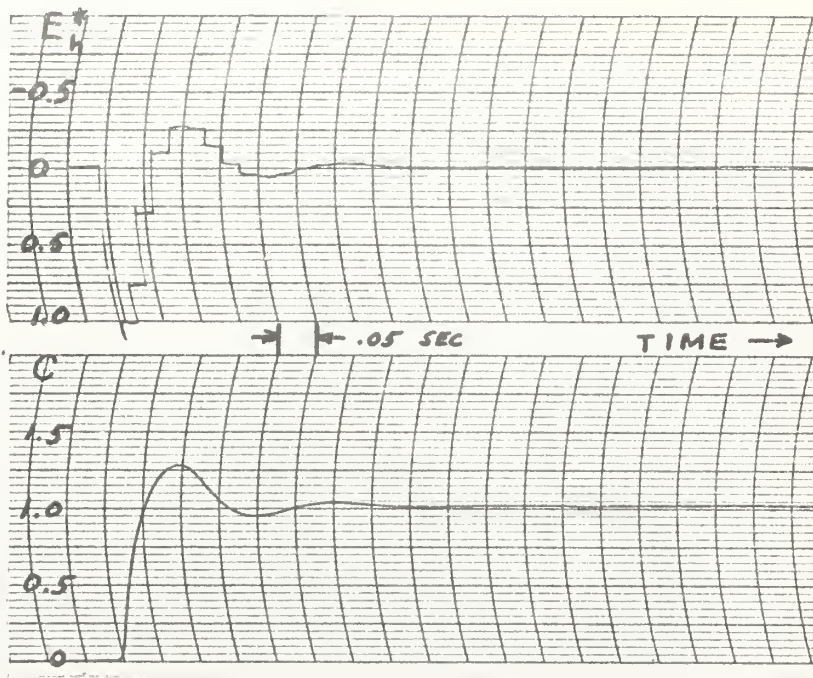
and if  $bT < 3.71$ , the relationship is:

$$0 < K \leq \frac{b^2(1 - e^{-bT})}{1 - e^{-bT}(1 + bT)}.$$

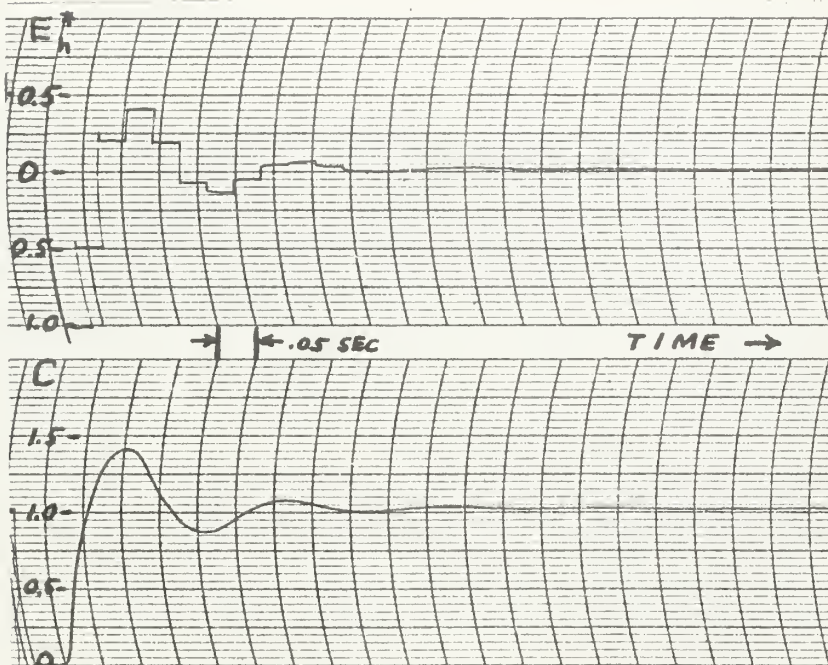
The Brush recordings of Figs. 5 and 6 illustrate a reasonable sampling period range for the type I system. Fig. 5(a) shows a reasonably fast sampling period that approximates the high frequency sampled closed loop response. Figs. 5(b) and 6(a) show intermediate sampling periods, and Fig. 6(b) illustrates a reasonably slow sampling period which is nearing the limit of T for stable response. Inspection of the z-plane root-locus diagrams shows that the type I system with  $bT < 3.71$  is more oscillatory near the limit of stability than is the type II system. This is also observed by comparing Figs. 2(c) and 6(b).

In the same manner as for the type II system, the minimum





(a)  $T = 0.023$  sec.

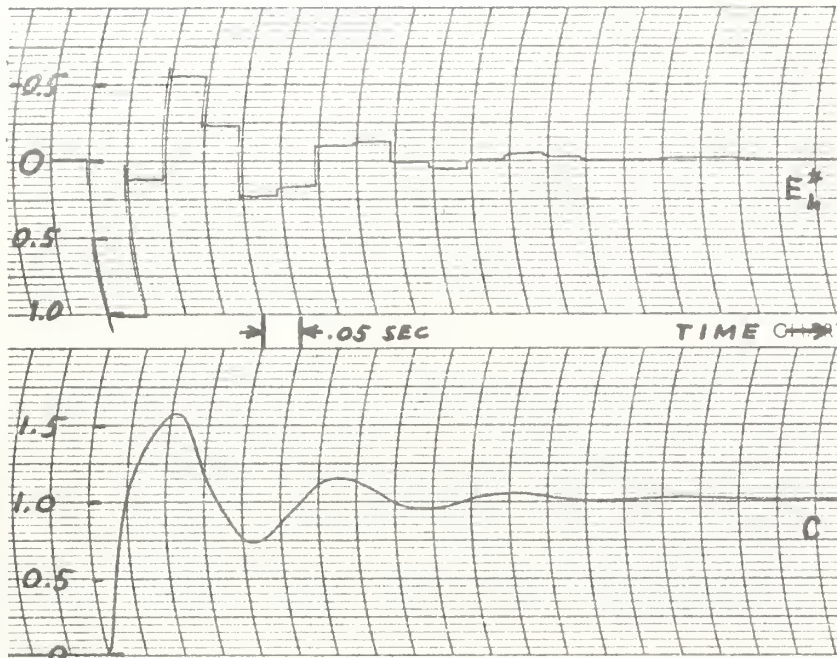


(b)  $T = 0.038$  sec.

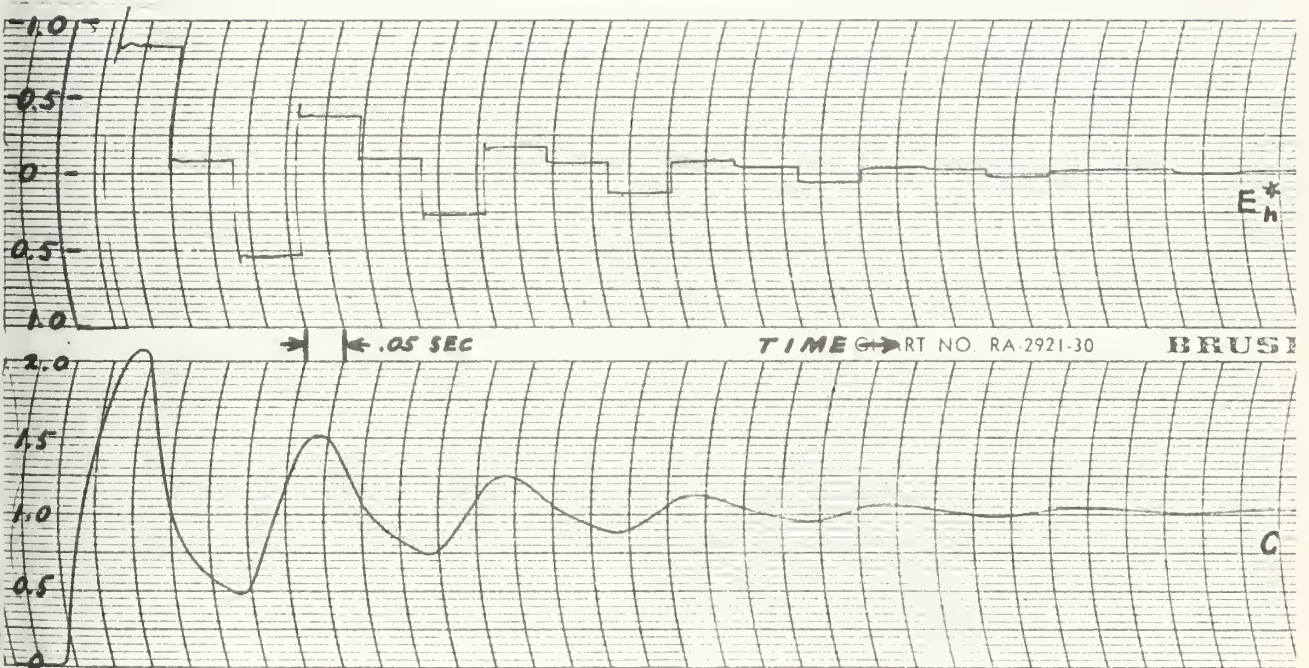
Fig. 5, Fixed sampling frequency response: Type I system,  
 $K = 1200$  ,  $b = 40$  .







(a)  $T = 0.050$  sec.



(b)  $T = 0.083$  sec.

Fig. 6. Fixed sampling frequency response: Type I system,  $K = 1200$ ,  $b = 40$ .



sampling period was determined by the largest value of  $T$  that produced continuous response characteristics. With system parameters  $b = 40$  and  $K = 1200$ , a reasonable range of  $T$  is given by  $.023 \leq T \leq .083$ . The system parameters  $b$  and  $K$  were chosen so that the range of the sampling period  $T$  would be similar to the range used for the type II system.

The graphs of Figs. 2, 4, 5, and 6 are all recordings of the closed loop system response to a unit step input and the corresponding output of the zero order hold. The analog computer solution is time scaled by the factor 20 so that each time unit on the Brush recordings represents .05 seconds of real time.

The purpose of this chapter was to demonstrate how the ranges of the various system parameters were determined and to justify the ranges so determined. The  $z$ -plane root-locus diagrams of Appendix F show the relationships of the open-loop gain, poles, and zeros to the system root locations. Treating  $T$  as a dependent variable allows a range of  $T$  to be determined, based on a stability criterion. This range of  $T$  determines an upper bound to the duration of the sample period. The lower bound to the sample period was determined by analog computer tests and could also be determined by bandwidth considerations. For any given set of system parameters, two fixed limits can be found so that: (1) it is not desirable to sample with longer periods than the upper bound to  $T$  because of stability considerations, and (2) it is not necessary to sample with shorter periods than the lower bound to  $T$  since



faster sampling provides relatively little additional information in the error channel to improve the system response. The upper and lower bounds to  $T$  determine the permissible range of variation of  $T$  when it is continuously or discretely varied during the transient periods of the system response as will be described in Chapter IV.



CHAPTER III  
VARIABLE FREQUENCY SAMPLING

The function of a sampler and hold in a servo system is to approximate a continuous signal as accurately as possible. One way to improve the accuracy of approximation is to increase the sampling frequency. Another way is to use a higher order hold than the zero-order hold which is generally used. Both these methods have distinct limitations. The first in demanding more performance of components and more time of communication channels, the second in more complicated circuitry. This chapter presents a method of improving the efficiency of a sampler-zero order hold combination by using variable frequency sampling. An efficient sampling system is defined to be one which satisfactorily approximates its input with a minimum number of samples over any period of time.

Fig. 7(a) shows the continuous input and sampled-held output of a sampler and zero-order hold using ordinary fixed frequency sampling. Since in the servo system the error signal is the input to the sampler, the symbols  $E$  and  $E_h^*$  will be used for the input and output of the sampler and hold. In this chapter the terms "input" and "output" will refer only to the signals in and out of the sampler and hold, not to the reference variable  $R$  and command variable  $C$  of the servo system. In Fig. 7(a) it can be seen that fixed-frequency sampling results in a better approximation of the input near the maximum of the





curve where the first derivative  $\dot{E}$  approaches zero than it does in the portion of rapid rise where  $\dot{E}$  is large.

Since in a servo system it is always the purpose to minimize  $E$ , the authors at first tried  $|E|$  as a frequency controlling variable. Fig. 7(b) demonstrates that attempting to control  $f_s$  as a function of  $|E|$  can actually decrease the efficiency of the system. When  $f_s$  is proportional to  $|E|$ , it can be seen that in the rapidly rising portion of the curve, sampling is too slow, and in the region of the maximum, the system is sampling unnecessarily fast.

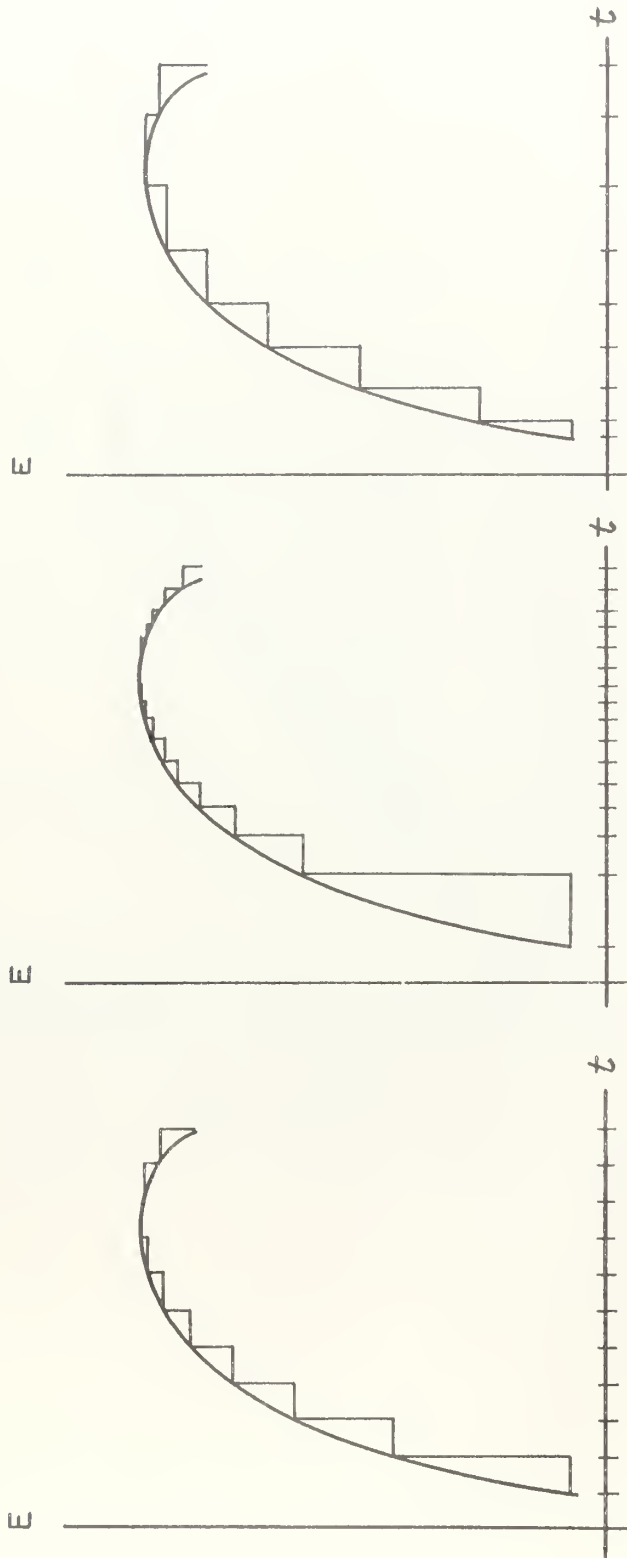
In Fig. 7(c),  $f_s$  is a function of  $\dot{E}$  and the accuracy of approximation appears to be nearly constant over the entire curve. This is the type of sampling frequency control found suitable for improving the efficiency.

Fig. 8 is a magnification of the input and output of the sampler over one sample period. The total area between the input and output in the sample period is the integral difference for one period:

$$\begin{aligned}
 ID &= \int_{t_i}^{t_{i+1}} (E - E_h^*) dt \\
 &= \int_0^{T_i} (E - E_h^*) dt
 \end{aligned}$$

In any successful sampled data servo system, the sampling frequency must be several times the highest system signal frequency of importance. Hence, it is assumed that  $\dot{E}$  does not vary radically during a sample period. Then a reasonable





(a) Fixed  $T$                       (b)  $T = T(E)$                       (c)  $T = T(\dot{E})$

Figure 7. Sampler and zero-order hold output.



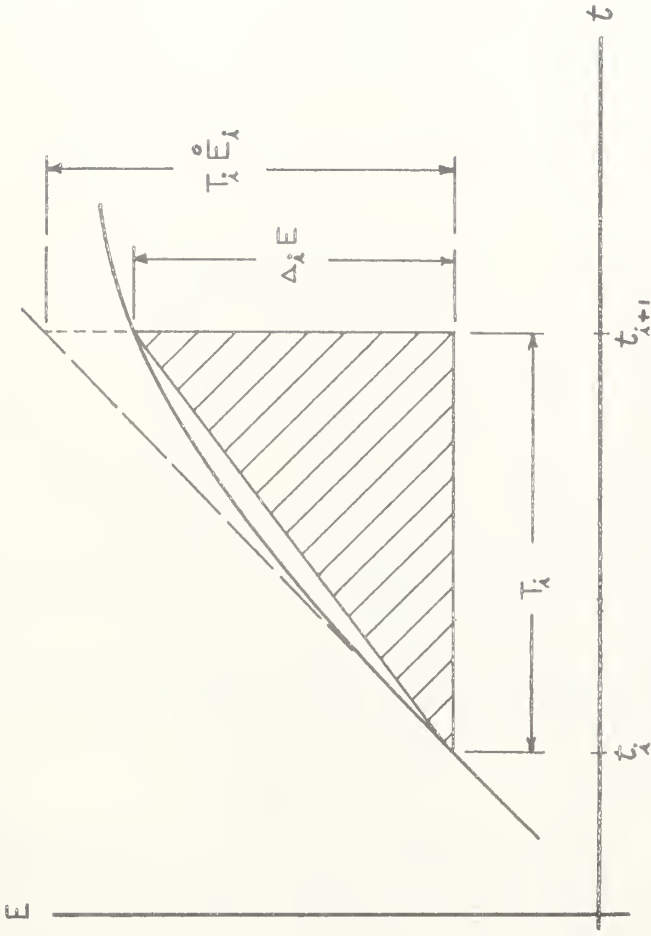


Figure 8. Integral difference (ID) over one sample period.



approximation of  $E$  over the period is a straight line approximation:

$$E = E_i + \dot{E}_a t$$

where  $\dot{E}_a$  is the first derivative of  $E$  at some instant  $a$  in the period. Fig. 8 shows approximations based on  $\dot{E}_i$  and a value of  $\bar{E}$  which has the same slope as the chord line.

Then an approximation of the integral difference is:

$$ID = \int_0^{T_i} (E_i + \dot{E}_i t - E_h^*) dt$$

but  $E_h^* = E_i$  over the entire period, hence:

$$ID = \int_0^{T_i} \dot{E}_i t dt = E_i \frac{T_i^2}{2}$$

Now if  $T$  is made a function of  $\dot{E}$  such that

$$T_i = \frac{C}{\sqrt{|\dot{E}_i|}} \quad \text{where } C \text{ is a constant,}$$

the integral difference per sample period will be a constant

$$ID = \pm \frac{C^2}{2},$$

the algebraic sign being the same as  $\dot{E}_i$ . Such a function for  $T_i$  is difficult to generate but can be approximated over a given range by simpler functions.

In Chapter II it was shown that, in general, a servo system has a usable range of  $T$  between upper and lower limits determined by the stability and the bandwidth of the system. The simplest way to control  $T$  was found to make it a linear function of  $|\dot{E}|$  between those limits.





$$T = T_{\max} - A \left| \dot{E} \right| \quad 0 < \left| \dot{E} \right| \leq \frac{T_{\max} - T_{\min}}{A}$$

$$T = T_{\min} \quad \left| \dot{E} \right| \geq \frac{T_{\max} - T_{\min}}{A}$$

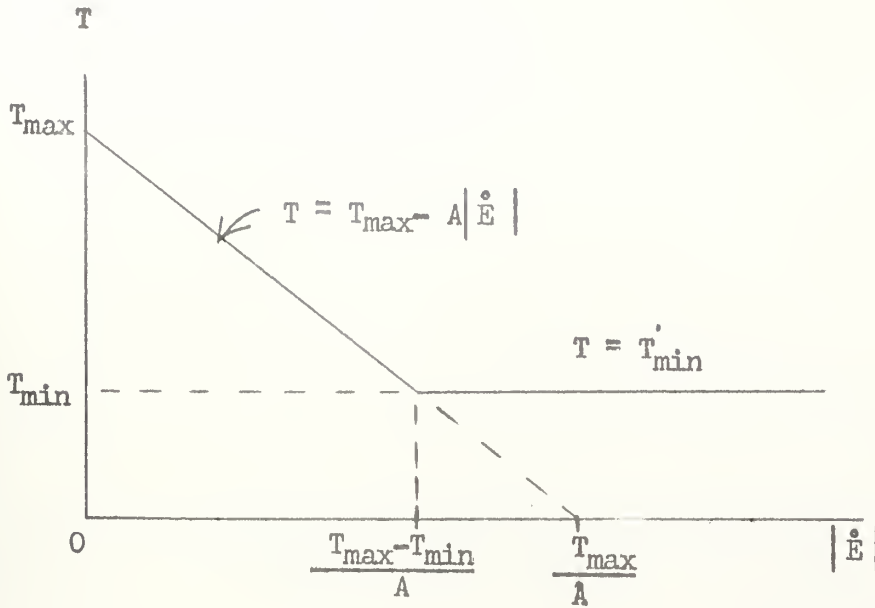
A method of generating this function using operational amplifiers is described in Appendices C and D.

The function is shown in Fig. 9(a). The ID per sample as a function of  $\left| \dot{E} \right|$  is sketched in Fig. 9(b). It can be seen that the ID can be held essentially constant over a limited range by using the linear function. In use with the simulated servo system, the linear function was found to improve the sampling efficiency as will be described in Chapter IV.

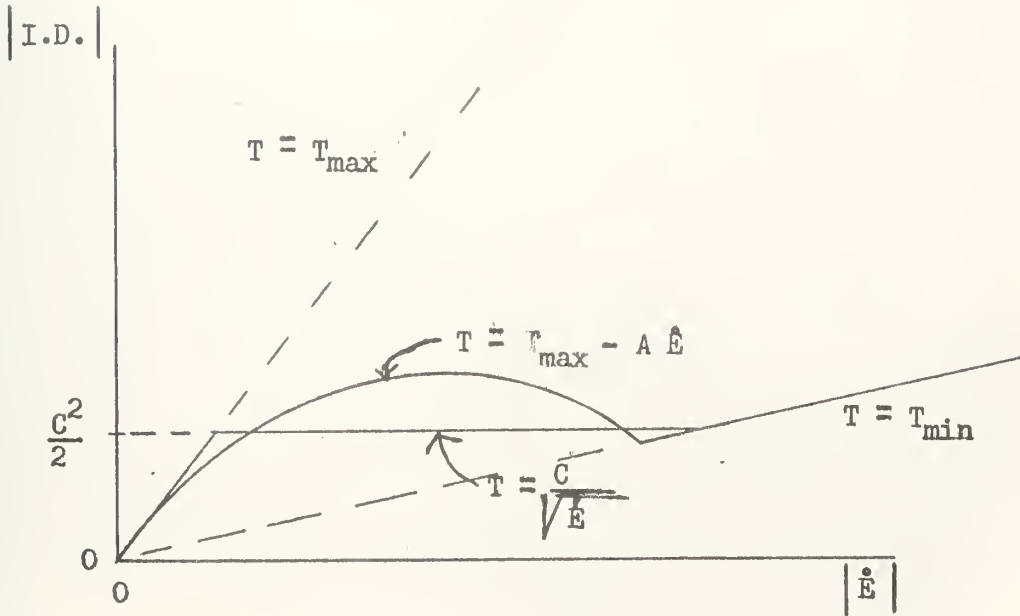
Another method of controlling the sampling frequency is by a number of fixed frequencies which are successively used as  $\left| \dot{E} \right|$  increases. A system using two discrete frequencies was found to improve efficiency and is also discussed in Chapter IV. Curves of T and ID as functions of  $\left| \dot{E} \right|$  are shown in Fig. 10.

Therefore, two methods of sampling frequency control have been investigated to improve efficiency. That these methods can be used to decrease the amount of sampling needed to control a servomechanism will be demonstrated in the next chapter.





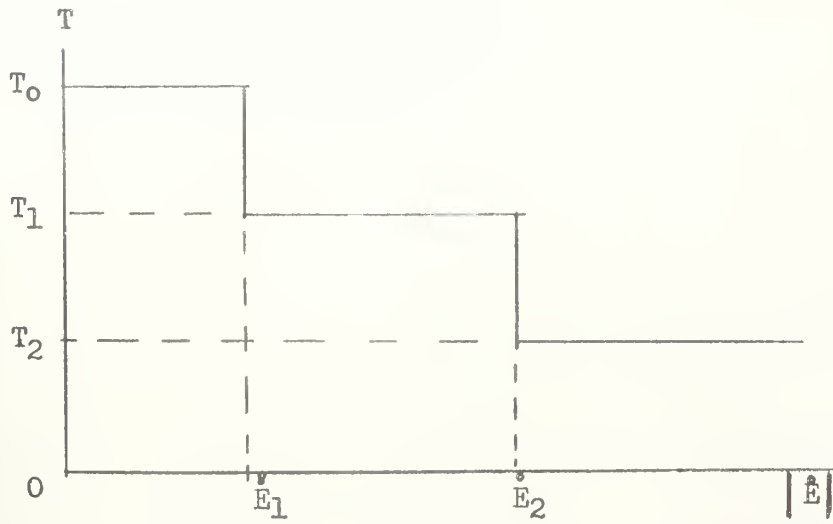
(a) Sample Period vs. Error Derivative.



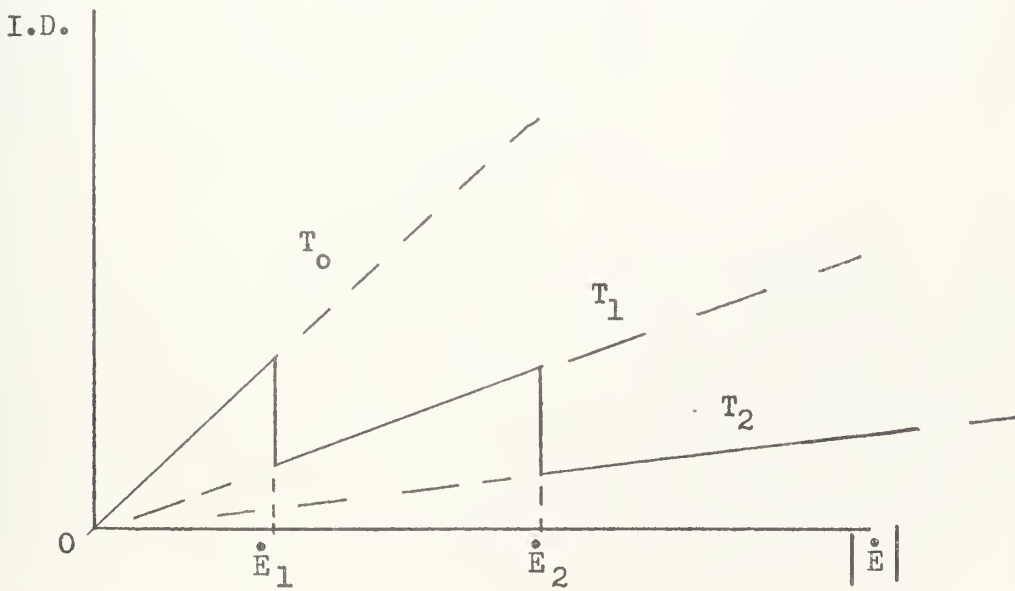
(b) Integral Difference per Sample Period vs. Error Derivative.

Fig. 9. Variable Sampling Frequency Control.





(a) Sample Period vs. Error Derivative.



(b) Integral Difference per Sample Period vs. Error Derivative.

Fig. 10. Discrete Sampling Frequency Control.



## CHAPTER IV

### SERVO SYSTEM WITH VARIABLE SAMPLING FREQUENCY

The characteristics of two sampled-data systems with fixed-frequency sampling were discussed in Chapter II. This chapter presents the characteristics of systems incorporating the variable-frequency sampling discussed in Chapter III. Fig. 11 is a block diagram of the system with the sampling-frequency controller. The principal method of analysis was an analog computer simulation.

In Chapter III it was seen that the integral difference between input and output of a sampler and zero-order hold could be controlled by varying the sampling period  $T$ . The method used was to make  $T$  a function of the first derivative of the input signal. Since the input to the sampler in this servo system is the error signal  $E$ :

$$T = T(|\dot{E}|) \quad (4-1)$$

Since the  $z$ -plane transfer function  $G(z)$  is a function of  $T$ , it becomes a function of  $|\dot{E}|$  when a variable frequency sampler is used. The servo system is then non-linear. Furthermore, the non-linearity is an unusually complicated one since the poles and zeroes of the transfer function, as well as the gain, are all functions of  $|\dot{E}|$ .

Because of the non-linearity of the system, an analog computer simulation was undertaken as being the most direct approach to the problem. With the simulation, all the non-linearities are accounted for by actually using a variable-





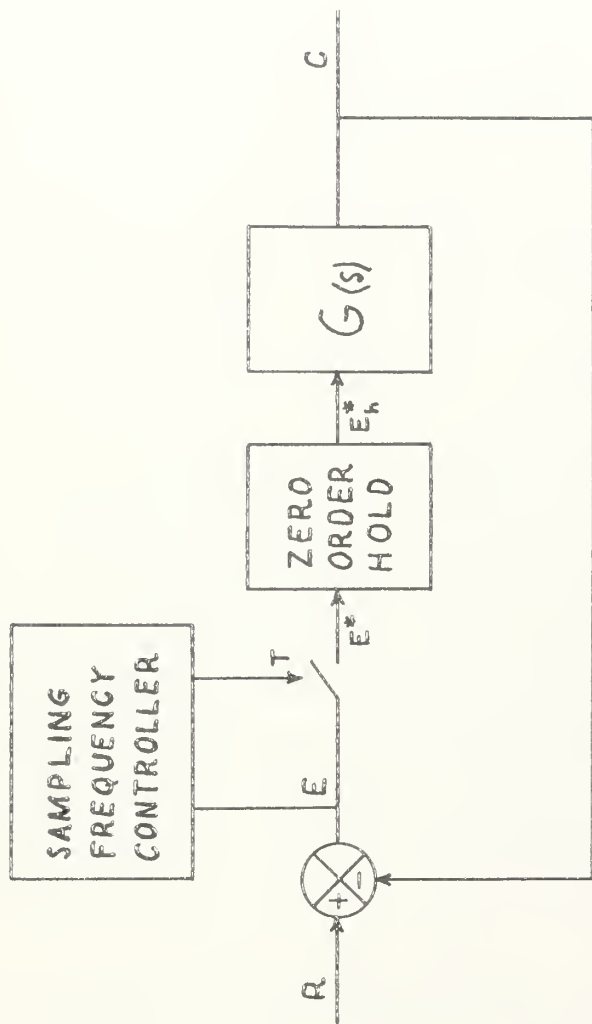


Figure 11. Block diagram of adaptive sampling frequency sampled-data control system.



frequency sampling system. Thus, the record of the computer output is a direct measure of system performance.

Since it was determined that the sampling frequency should increase as a function of the absolute value of the first time-derivative of the error signal, the controller consisted of a differentiator, an absolute value detector, shaping circuits, and a variable frequency oscillator. The function generated for control was:

$$T = T_{\max} - A \left| \dot{E} \right| \quad 0 \leq \left| \dot{E} \right| \leq \frac{T_{\max} - T_{\min}}{A}$$

$$T = T_{\min} \quad \left| \dot{E} \right| \geq \frac{T_{\max} - T_{\min}}{A}$$

Fig. 12 is a block diagram showing these components in the system. Another method of control found to be satisfactory was to use two discrete frequencies instead of continuously variable frequencies. Fig. 13 is a block diagram of the system with a discrete frequency controller which switches frequencies at  $\left| \dot{E} \right| = \left| \dot{E}_1 \right|$ . The details of the analog simulation circuits are described in Appendices A through E.

The two systems analyzed for fixed frequency sampling in Chapter II had acceptable response characteristics as continuous systems. For each system a pair of sampling frequency limits were found such that above the upper limit, no improvement in response occurred and below the lower limit, the system was unstable. In the analog computer study, a fixed frequency between these limits was chosen such that



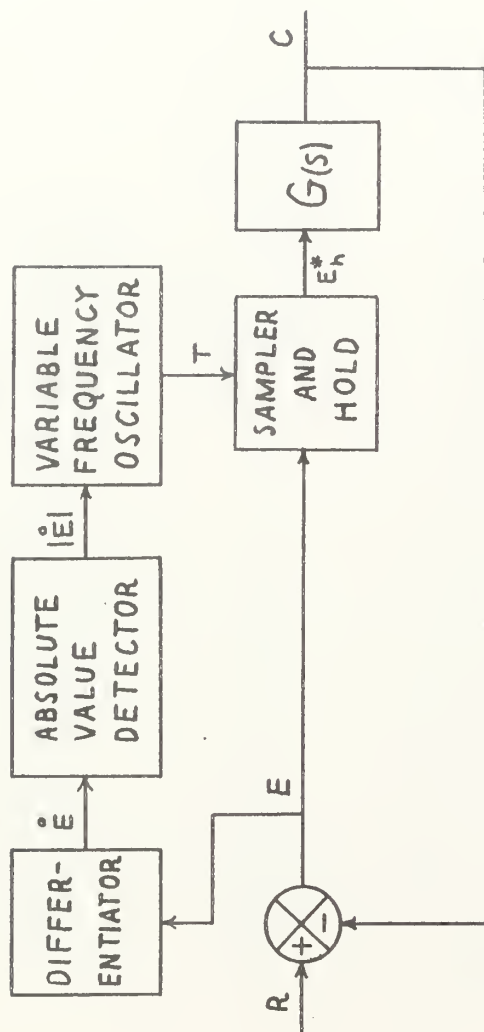


Figure 12. Block diagram of  $\dot{E}$  dependent variable sampling frequency control.



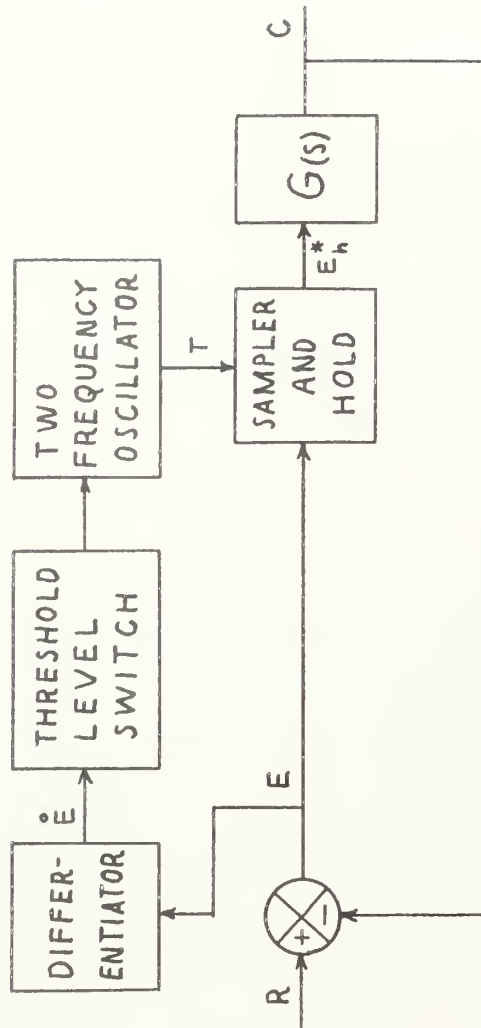


Figure 13. Block diagram of  $\dot{E}$  dependent discrete frequency control.





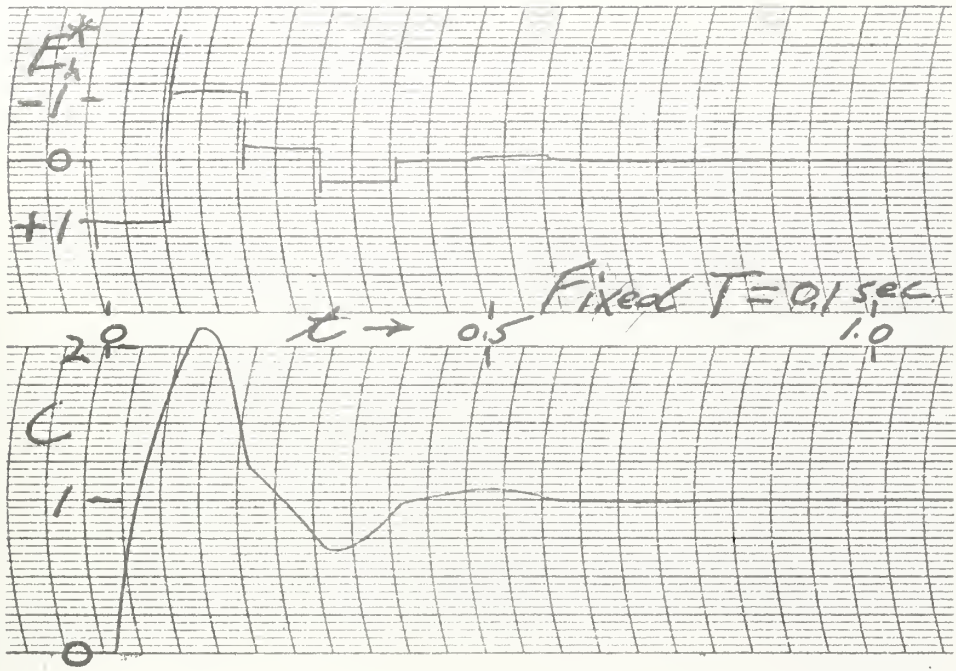
system performance was satisfactory, and only slightly more oscillatory than the comparable continuous system. Its performance was then used as a standard against which the variable frequency and multiple frequency systems were compared. If the variable  $f_s$  system could produce similar response with fewer samples per unit time, then it was said to be more efficient.

Fig. 14 is a series of recordings of the response of the type II system to a unit step input. Table 4-1 is a summary of the response characteristics determined from the recordings. For each variable period run  $T_{\max} = 0.1$  sec.,  $T_{\min} = 0.05$  sec. Examples include runs at constant  $T_{\min}$  and  $T_{\max}$ , bi-frequency runs switching from  $T_{\max}$  to  $T_{\min}$  at  $\left| \dot{E}_1 \right|$ , a run using continuous control between  $T_{\min}$  and  $T_{\max}$ , and three high-frequency runs (i, j, k) for comparison.

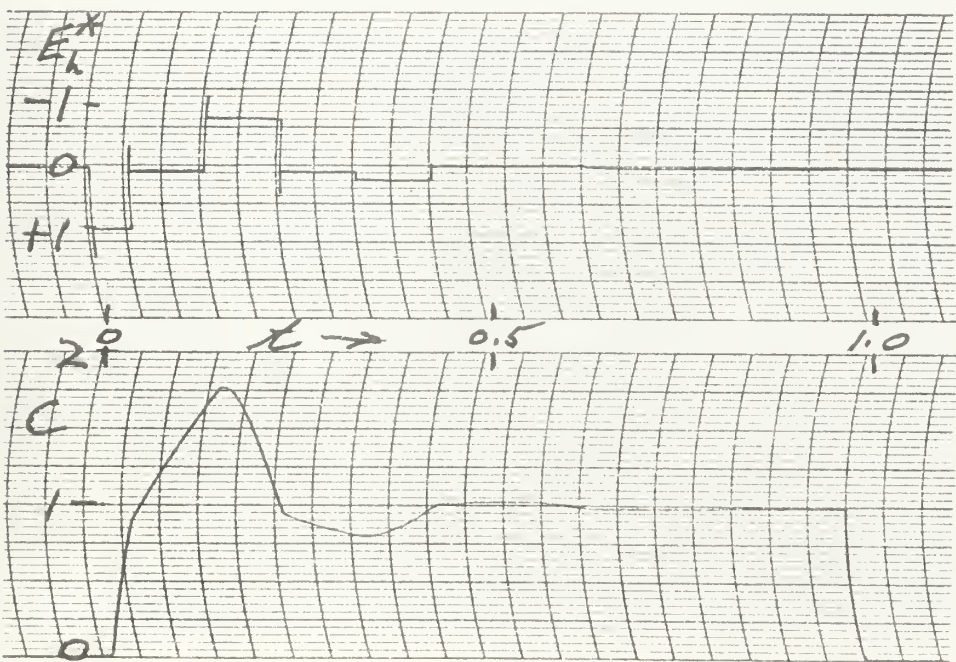
Run (g) having  $T = T_{\min}$  was used as the standard of performance. In Chapter II, it was shown that the response at  $T = 0.05$  sec. closely approximates the response of the continuous system. The variable and bi-frequency systems all sample at half the frequency of the standard system when  $\dot{E} = 0$ , thus sampling is reduced by 50% under quiescent steady-state conditions.

The settling time for response to a step input is approximately 0.5 sec. for each type of control. Over the settling time, sampling has been reduced 10% using bi-frequency sampling in run (f) and 20% using variable frequency in run (h). Both these runs demonstrate a reduction





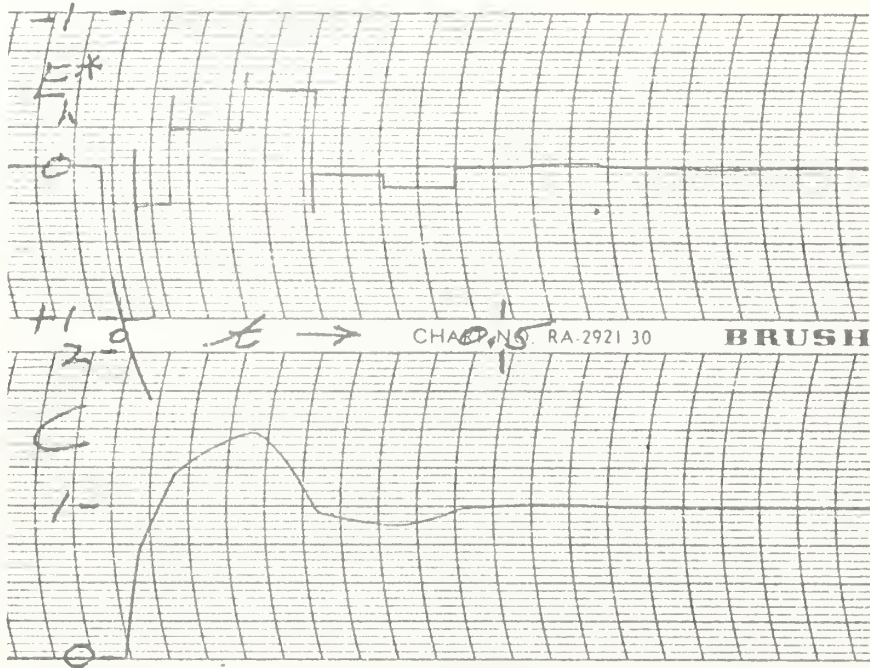
(a)  $T = 0.1$  sec.



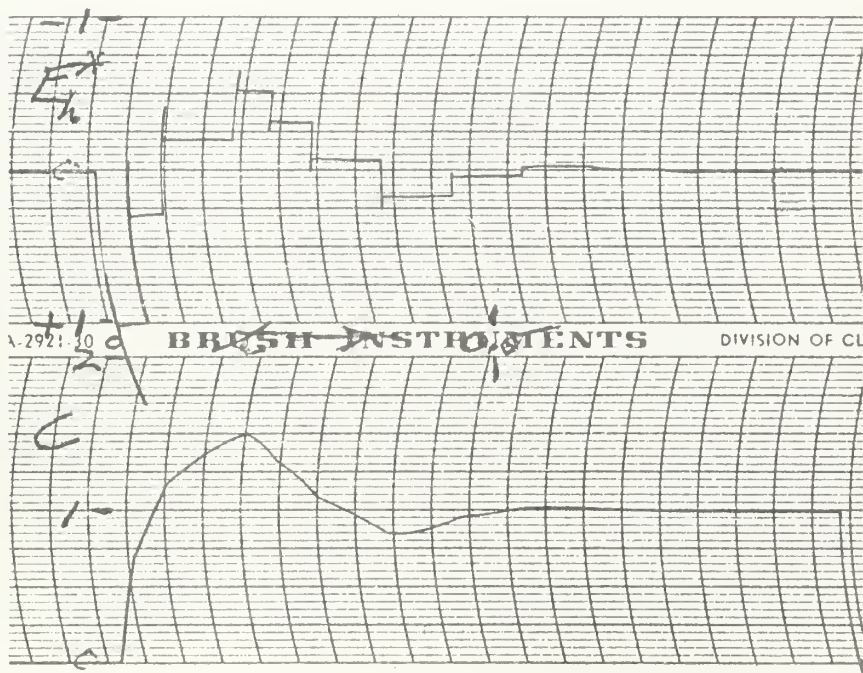
(b)  $T_0 = 0.1$  sec. ;  $T_1 = 0.05$  sec. at  $|\dot{E}| = 20$  rad/sec.

Fig. 14. Type II Servo responses to unit step.





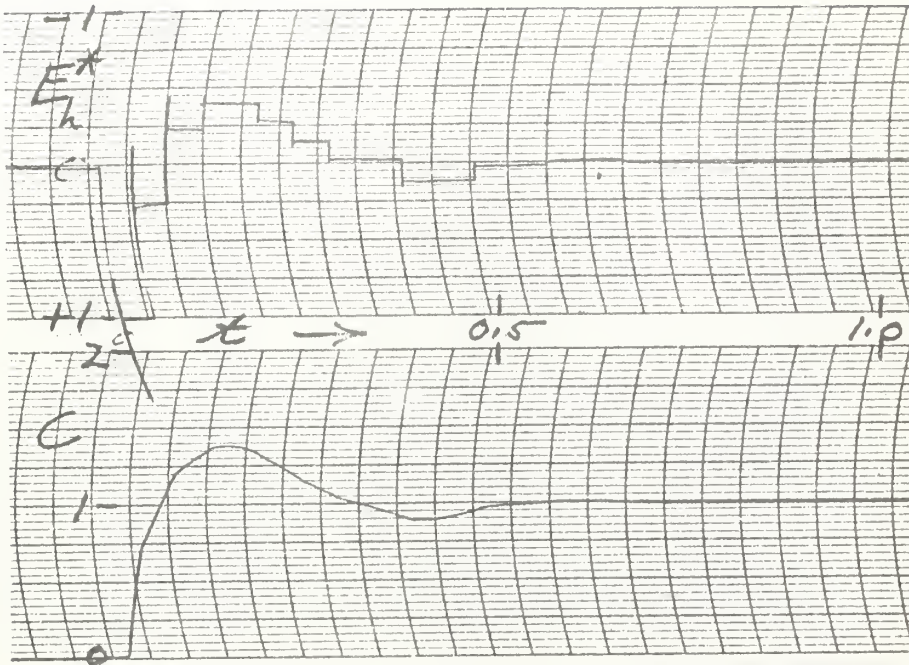
(c)  $T_0 = 0.1 \text{ sec.}$  ;  $T_1 = 0.05 \text{ sec.}$  at  $|\dot{E}| \geq 10 \text{ rad/sec.}$



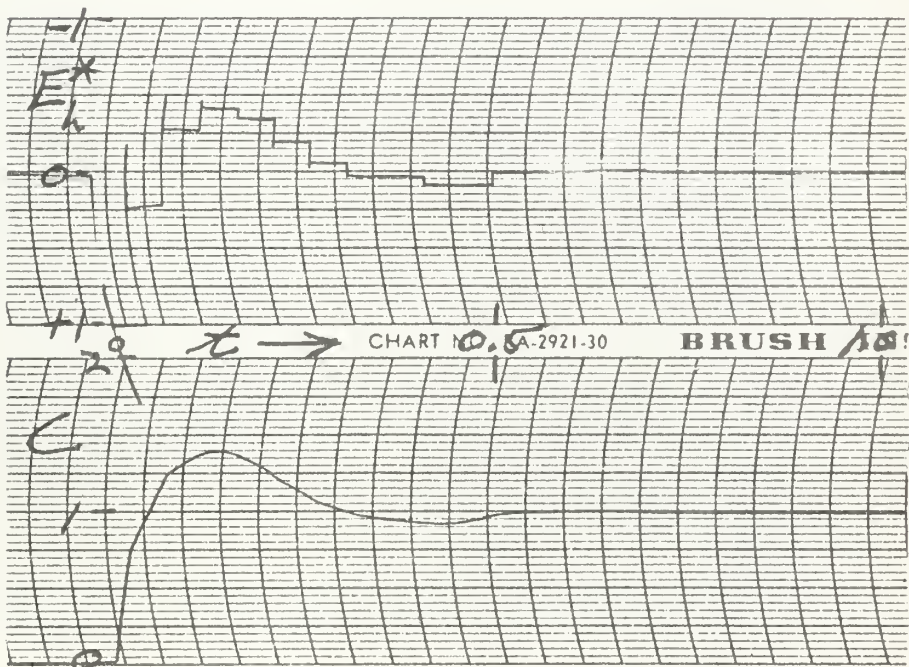
(d)  $T_0 = 0.1 \text{ sec.}$  ;  $T_1 = 0.05 \text{ sec.}$  at  $|\dot{E}| \geq 5.0 \text{ rad/sec.}$

Fig. 14. Type II SERVO response to unit step.





(e)  $T_0 = 0.1$  sec.;  $T_1 = 0.05$  sec. at  $|\dot{E}| = 2.50$  rad/sec.

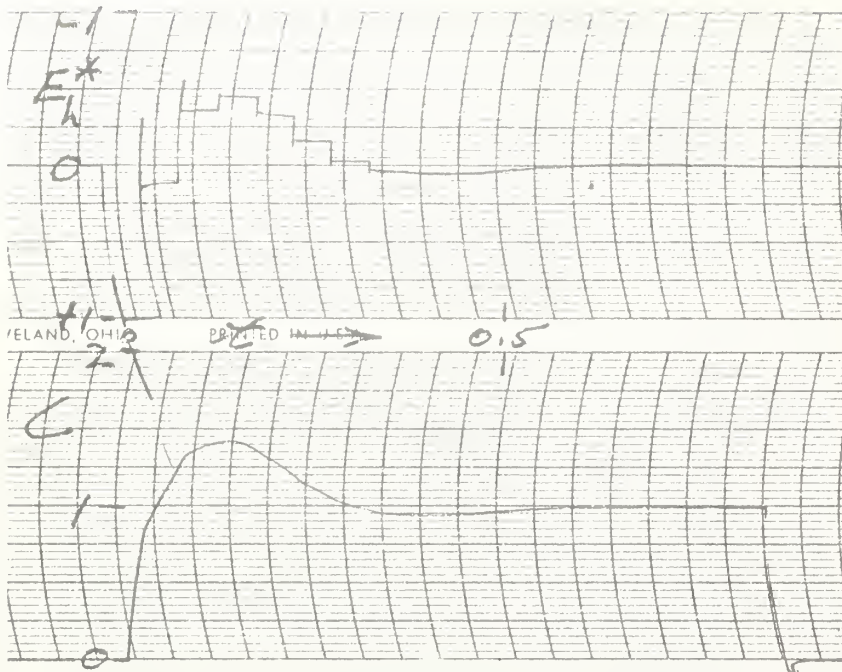


(f)  $T_0 = 0.1$  sec.;  $T_1 = 0.05$  sec. at  $|\dot{E}| = 1.250$  rad/sec.

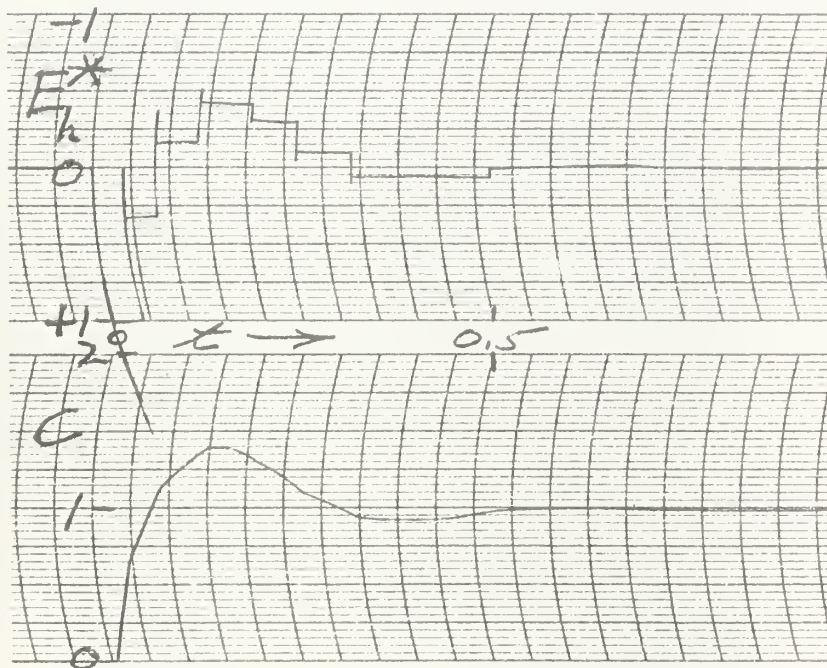
Fig. 14. Type II Servo response to unit step.







(g)  $T = 0.05$  sec.

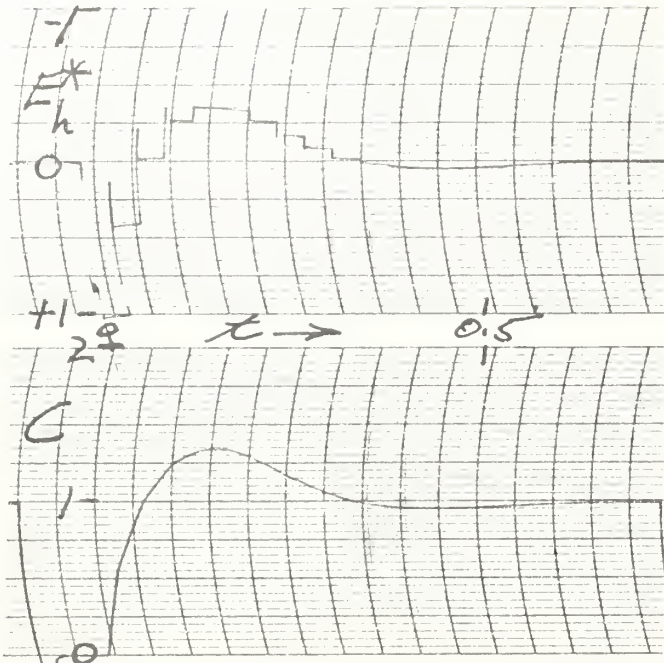


(h)  $T_{\max} = 0.1$  sec.;  $T_{\min} = 0.05$  sec.

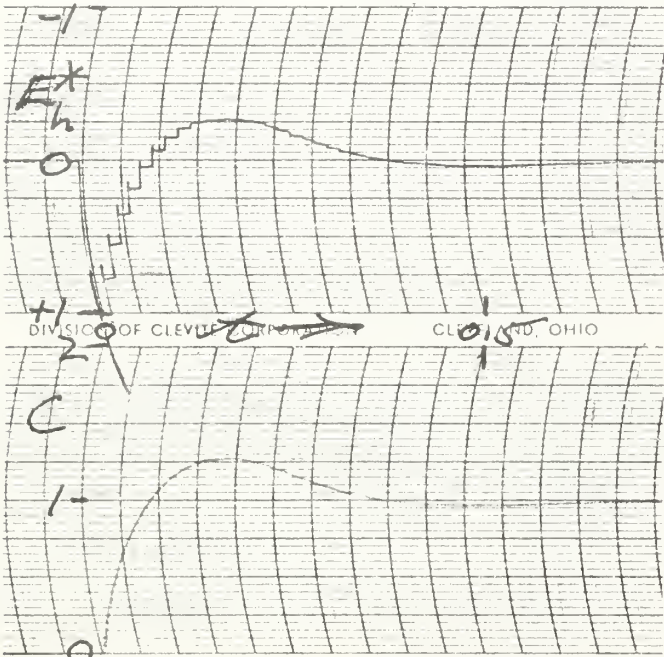
$A = 0.005$  ; (Eqn. 4-2)

Fig. 14. Type II Servo response to unit step.

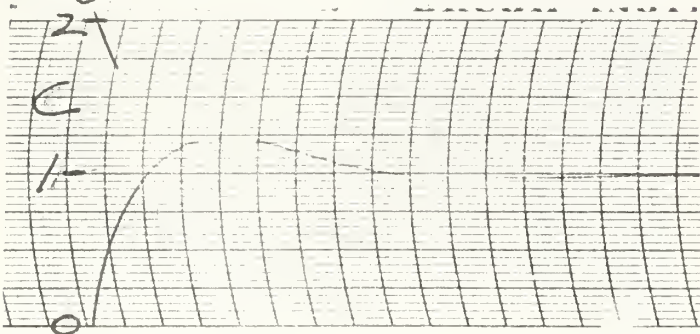




(i)  $T = 0.036$  sec.



(j)  $T = 0.016$  sec.



(k)  $T < 0.005$  sec.

Fig. 14. Type II Servo response to unit step.



in sampling while maintaining essentially the same response characteristics as the standard. By setting  $\left| \dot{E}_1 \right|$  at higher levels, the number of samples over the settling period is reduced at the expense of higher peak overshoots. Specifications and system requirements would dictate which type of control and what sensitivity to use in a particular case. Results with the type I system were similar over the same type of frequency range.

It can be seen that the variable frequency control system definitely accomplishes its purpose of more efficient sampling. In general, the continuously variable control system was more efficient than the two-frequency control, but even the latter was a distinct improvement over constant-frequency sampling.

Table 4-1

Comparative Responses to 1 rad. Step Input. (From Fig. 14.)

Sample Period T	Samples over		Overshoot	Undershoot
	0.5 sec	1.0 sec		
a. $T_o = T_{max} = 0.1$ sec.	5	10	110%	33%
b. $\left  \dot{E}_1 \right  = 20$ rad/sec.	6	11	75	20
c. " 10 "	7	12	50	12
d. " 5.0 "	8	13	50	20
e. " 2.5 "	8.5	13.5	40	10
f. " 1.25 "	9	14	40	8
g. $T_1 = T_{min} = 0.05$ sec.	10	20	40	6
h. $T = T_o - 0.005 \left  \ddot{E} \right $ sec. (Eqn. 4-2)	8	13	40	8



CHAPTER V  
ADAPTABILITY

This chapter will discuss the adaptive qualities of the variable sampling frequency system to variations of plant parameters, i.e., open loop system pole or zero variations. A second consideration will be whether the variable sampling frequency system can be programmed to be adaptive to plant parameter variations.

Consider first the adaptivity of the variable sampling frequency system to plant parameter variations. The basic z-plane root-locus relationships are discussed in Appendix F. It is seen that this system is inherently adaptive to parametric variations in the sense that the variable sampling frequency will compensate for the parametric variations which increase or decrease the error rate.

The sampling frequency is controlled by a function of the first derivative of the error. In the sense that the varying plant parameter will cause a variation of the error derivative, then the sampling frequency will be adaptive to this parameter variation. That is, if the parameter is varying or varied in such a manner as to reduce the error derivative, then the sampler will sample more slowly; and if the parameter variation increases the error derivative, then the sampler will sample more rapidly.

Consider the situation where it is possible to measure the changes of a varying system parameter and, as a result of this information, correspondingly change the value of the





open loop gain or the sampling frequency. Specifically, consider the type II system with a fixed sampling period  $T$ , where

$$G(z) = KT\left(1 + \frac{aT}{2}\right) \left[ \frac{z + \frac{aT - 2}{aT + 2}}{(z - 1)^2} \right]$$

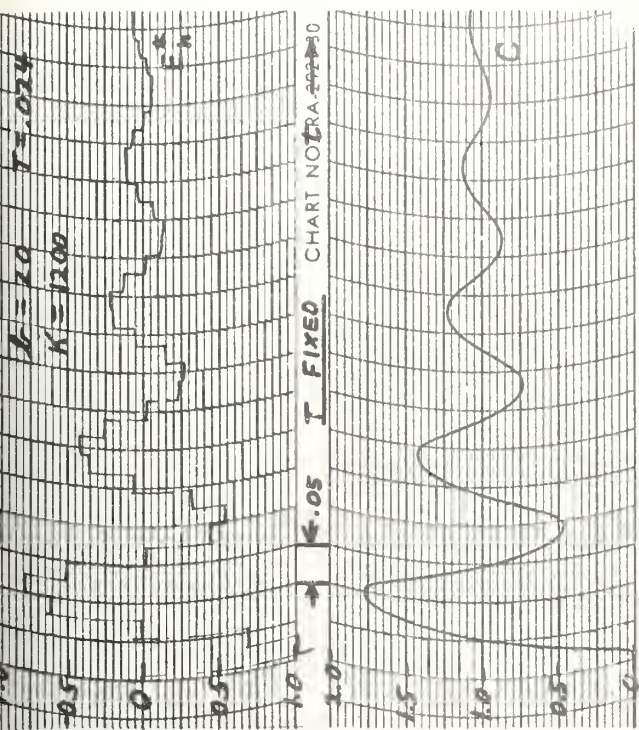
Let the  $s$ -plane open-loop zero be changed from  $a$  to  $c_1 a$  where  $c_1$  is a positive real constant. As a compensation investigation, let  $T$  be changed from  $T$  to  $T/c_1$ , and  $K$  be changed from  $K$  to  $c_1 K$ . Therefore, the products  $aT$  and  $KT$  are unchanged, and the  $z$  transform  $G(z)$  is exactly the same expression as before the disturbance  $c_1$  was introduced. However, the real time output response has been changed. Since the  $z$  transform is unchanged, it is seen that the amplitude of the  $i^{\text{th}}$  sample, where ( $i = 0, 1, 2, \dots, n$ ) is unchanged, however, the  $i^{\text{th}}$  sample now occurs at real time  $t = (T)(i)/c_1$  instead of at  $t = (T)(i)$  as before. Therefore, this method of compensation preserves all relative response amplitudes but changes the time of the response, increasing the speed of response as the zero (or pole of the type I system) becomes larger in value and decreases the speed of response as the zero (or pole of the type I system) becomes smaller in value.

If it is desired to maintain exactly the same response characteristics while the open-loop zero value changes, then  $T$  and  $K$  may be varied in some programmed manner to achieve the desired response, but such an investigation is beyond the scope of this thesis.

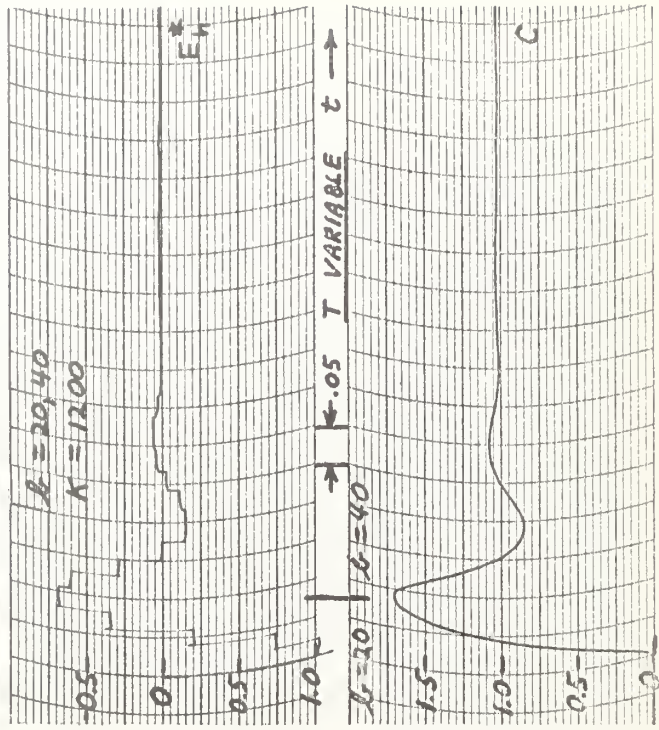


Fig. 15 illustrates the effect of introducing a change in the value of the type I system open-loop pole. Fig. 15(a) shows the variable sampling frequency response where  $b = 40$ ,  $K = 1200$ , and  $.03 \leq T \leq .07$ . The response has essentially two overshoots and two undershoots. Fig. 15(b) shows fixed sampling frequency response where  $b = 20$ ,  $K = 1200$ , and  $T = .024$ . The peak overshoot is 77% and the response is relatively oscillatory. Fig. 15(c) shows the system response where  $b = 20$  ( $0 \leq t \leq .090$ ), then  $b = 40$  ( $.090 < t$ ), and  $K = 1200$  with fixed  $T$  of  $T = .025$ . The peak overshoot is 80% because of the  $b = 20$  value, and after  $t = .090$ ,  $b = 40$  and the oscillation damps out quickly as in (a). The peak overshoot is greater in (c) than in (b) because the sampling period in (c) is longer than the period in (b). In Fig. 15(d) the system is again  $b = 20$  ( $0 \leq t \leq .090$ ), then  $b = 40$  ( $.090 < t$ ) and  $K = 1200$ , with variable frequency sampling in the range  $.019 \leq T \leq .045$ . Comparing (d) with (c), the peak overshoot is reduced from 80% to 70% as a result of the higher sampling frequency allowable, and the peak undershoot is reduced from 20% to 15% because of the higher frequency sampling. The response in (d) has essentially two overshoots and two undershoots as in the case (a). In 0.5 seconds the transient has died out in both the fixed sampling case (c) and the variable sampling case (d). It is seen that the response in the variable sampling case with plant parameter change has less peak overshoot and less peak undershoot than the fixed sampling case and has achieved the better

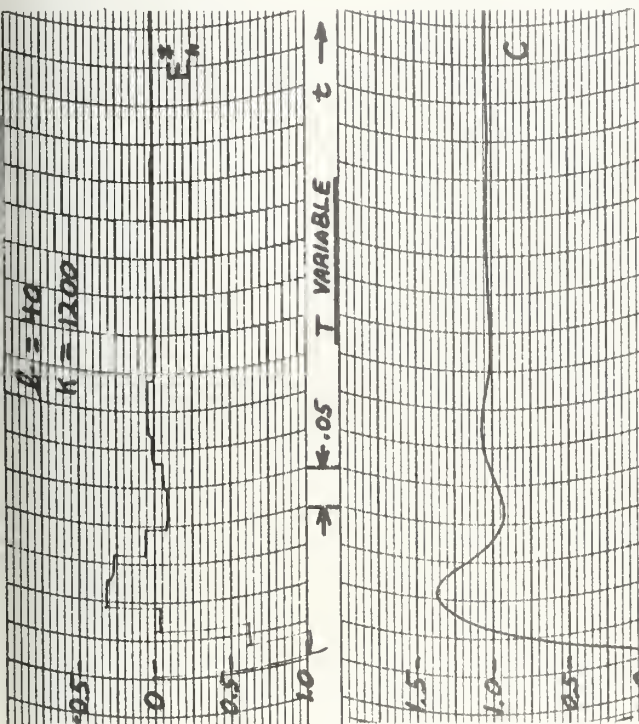




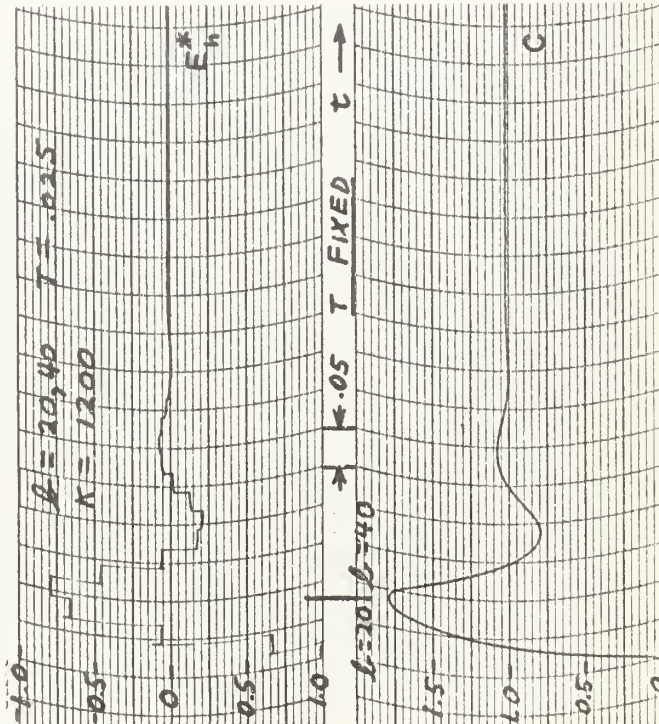
(a)



(b)



(c)



(d)

Fig. 15. Effect of varying open loop pole in type I system.



response with 17 samples in 0.5 seconds, while the fixed frequency sampler sampled 20 times in 0.5 seconds.

The variable frequency sampler is controlled by the error derivative with the sampling period  $T$  varying over a given range. The sampler is not aware of the source of the disturbance causing the error derivative value, be it input signal, noise, system parameter variation, or load torque; the sampling frequency is determined within its range by the error derivative value and, in this sense, the variable frequency sampling system is adaptive to all error-producing disturbances.





## CHAPTER VI

### CONCLUSIONS AND RECOMMENDATIONS

This thesis has described a method of adaptive sampling frequency control for sampled-data servomechanisms. In the system described, the minimum sampling frequency for stability was about 50% of the sampling frequency necessary for the best transient response. Therefore, with the adaptive sampling frequency control generating a variable frequency between those two limits, the maximum possible reduction in the number of samples needed over a given period of time is 50% if the system is undisturbed during this time. The reduction in number of samples over the settling time of the system to a step input was found to be about 20%. It would, therefore, seem conservative to estimate an overall reduction in number of samples required of about 25%, or half the maximum possible reduction, for a system which is subject to disturbances relatively often but not continuously.

Therefore, an approximate method of determining the percent reduction in number of samples using the adaptive sampling control is as follows:

Determine the minimum sampling frequency for the system from absolute stability requirements and the maximum sampling frequency from transient requirements, bandwidth considerations, or comparison with a comparable continuous system. If these two frequencies are set as the limits of variable  $f_s$  in the adaptive system, an approximate estimate of the average



number of samples required over a long time is:

$$N = \frac{f_{\max} + f_{\min}}{2} t$$

If the system is subject to few disturbances,  $N$  approaches  $f_{\min} t$ . On the other hand, if the system is continually disturbed,  $N$  will increase toward  $f_{\max} t$  as an upper bound. In no case will the number of samples required be greater than for the fixed  $f_s$  system. Even in a constantly disturbed system,  $\dot{E} = 0$  at each maximum and minimum excursion of  $E$  and some reduction in sampling will occur.

Recommendations for future investigation:

1. Control the voltage controlled oscillator, the multivibrator discussed in Appendix D, by the other methods described therein; namely, by two values of  $|\dot{E}|$  in the sample period and by continuously measuring  $|\dot{E}|$ . Additional analog stages could be used for inverting and biasing  $|\dot{E}|$  instead of the bias battery used here.

2. Use an electronic function generator to generate any number of functions of  $|\dot{E}|$  to control the sample period. It is possible that functions other than the simple ones used here might provide more efficient sampling control.

3. Approximate  $|\dot{E}|$  by backward differences taken on the output of the sampler and hold. In many systems, the continuous input to the sampler might not be readily available. Since the sample period is variable, complications can be foreseen but the technique, if successful, would be directly applicable to digital systems.



4. Test the system in various simulated applications and determine the long-time average saving in the number of samples required.

5. Develop the theory of variable frequency sampling. The theory of fixed sampling-frequency sampled-data systems has been used in this project. Process control theory, information theory, and statistical sampling theory all might aid in the development of a theory for this type of system.



## REFERENCES

1. Friedland, B. "A Technique for the Analysis of Time-Varying Sampled-Data Systems," Trans. AIEE, Vol. 76, Pt. II, (January, 1957), pp. 407-413.
2. Hufnagel, R. E. "Analysis of Cyclic Rate Sampled-Data Feedback Control Systems," Trans. AIEE, Vol. 77, Pt. II, (1958), pp. 421-423.
3. Tou, J. T. Digital and Sampled-Data Control Systems, McGraw-Hill Book Company, Inc., 1959.
4. Jury, E. I. and F. J. Mullin. "The Analysis of Sampled-Data Control Systems with A Periodically Time-Varying Sampling Rate," IRE Trans. on Automatic Control, Vol. AC-4, No. 1, May, 1959.
5. Hufnagel, R. E. "Analysis of Aperiodically-Sampled-Data Feedback Control Systems," (unpublished Doctoral dissertation, Cornell University, June, 1959).
6. Morrill, C. D. and R. V. Baum. "Diode Limiters Simulate Mechanical Phenomena," Electronics, Vol. 25, Pt. 4, (October-December, 1952), pp. 122-126.
7. Korn, G. A. and T. M. Korn. Electronic Analog Computers, second edition, McGraw-Hill Book Company, Inc., 1956.





## BIBLIOGRAPHY

- Aseeltine, J. A. and R. A. Nesbit. "The Incremental Phase Plane for Nonlinear Sampled-Data Systems," Space Technology Laboratories, Inc., University of California at Los Angeles, Los Angeles, California, March 21, 1960.
- Dorf, R. A. Sampled-Data Lecture Notes, U. S. Naval Postgraduate School, 1960.
- Grabbe, E. M. and others. Handbook of Automation, Computation, and Control, Vol. 2, John Wiley & Sons, Inc., 1959.
- Jury, E. I. Sampled-Data Control Systems, John Wiley & Sons, Inc., 1958.
- Ragazzini, J. R. and G. F. Franklin. Sampled-Data Control Systems, McGraw-Hill Book Company, Inc., 1958.
- Thaler, G. J. and R. G. Brown. Analysis and Design of Feedback Control Systems, McGraw-Hill Book Company, Inc.,
- Truxal, J. G. Automatic Feedback Control System Synthesis, McGraw-Hill Book Company, Inc., 1955.
- Truxal, J. G. (ed.). Control Engineers' Handbook, McGraw-Hill Book Company, Inc., 1958.
- Wheeler, R. C. H. Basic Theory of the Electronic Analog Computer, Donner Scientific Company, 1958.



## APPENDIX A

### COMPLETE ANALOG COMPUTER SIMULATION

The complete analog computer setup is shown in Fig. A-1. Time scaling of 20:1 was used throughout, i.e., 20 seconds of computer time corresponds to 1 second in the simulated servo system.

The basic sampled data servo system is simulated by amplifiers 8 through 12. The control circuits for the sampler are incorporated in amplifiers 1 through 7. A further breakdown of the system into its functional parts follows.

Amplifiers 8 and 10 through 12 are standard adders, sign changers, and integrators commonly used in analog simulation of servo systems. Amplifier 9 and the associated relay circuit make up the sampler and zero-order hold simulator. This circuit samples the continuous error signal from amplifier 8 at intervals determined by the control circuits and holds the sampled voltage as a constant output to the next amplifier until the next sample occurs. At the time of the next sample, the output of amplifier 9 jumps to the new sampled value and again holds it constant. Appendix B contains a detailed explanation of the operation of the sampler and hold circuit.

The first stage of the sampling control circuits is amplifier 1 which is a differentiator. It provides the first derivative of the continuous error signal which is the output of summing amplifier 8 in the main channel of the simulated servo system. Amplifiers 2 and 3 are the precision absolute value detector and signal shaping circuits. They take the



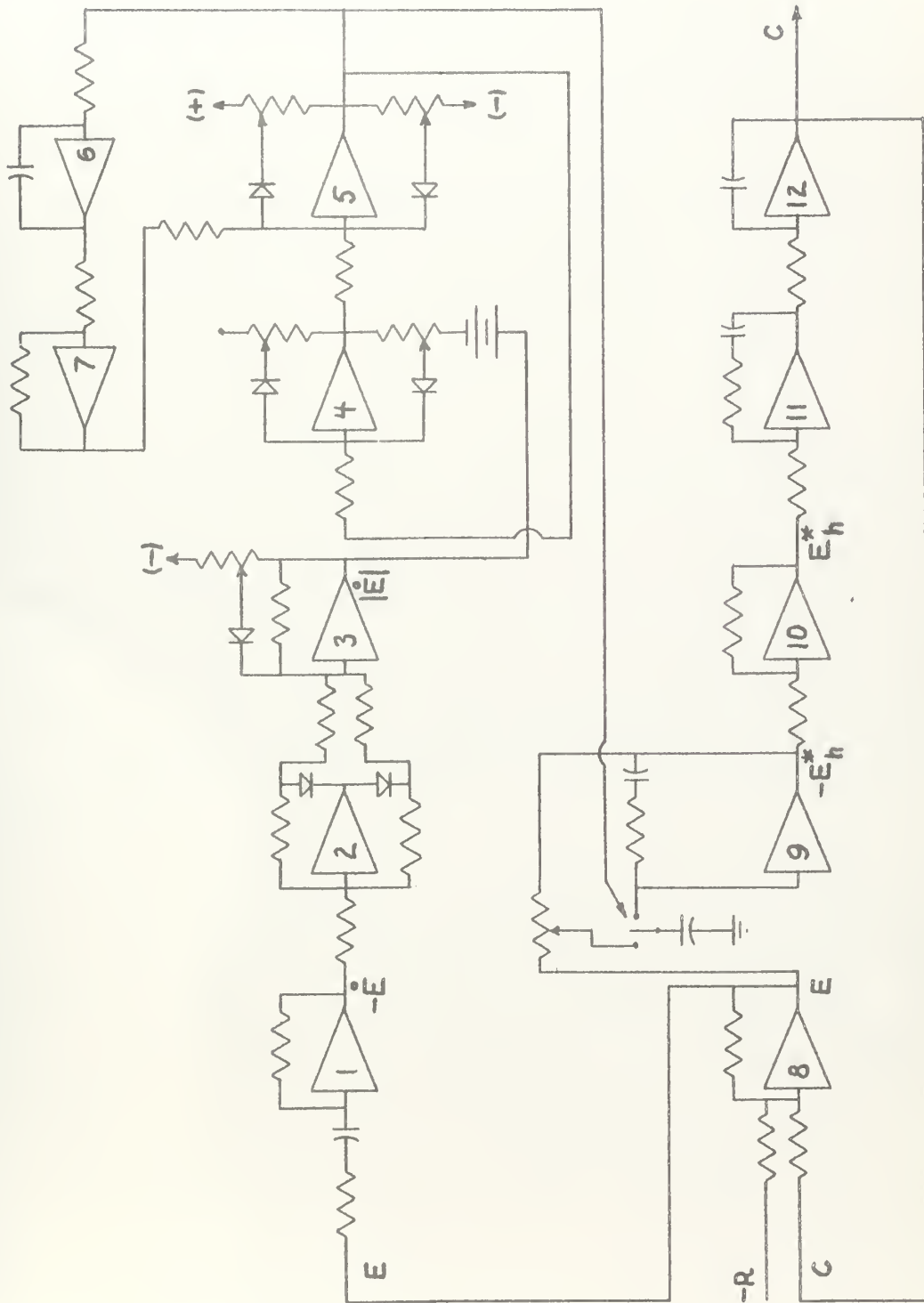


Figure A-1. Analog simulation circuit.



output of amplifier 1 is the first derivative of the error signal, detect the absolute magnitude of it, and further shape the signal as required for the variable frequency oscillator. The circuits associated with amplifiers 1 through 3 are explained in detail in Appendix C.

Amplifiers 4 through 7 are the voltage controlled variable frequency oscillator. The frequency of the square wave output of amplifier 5 is a function of the input voltage to one of the diode circuits associated with amplifier 4. The operation of the oscillator is explained in detail in Appendix D. The oscillator output is used to operate the transistorized relay control of the sampler and hold circuit at amplifier 9 back in the main channel of the servo system. Thus, a signal which is a function of the servo system error signal is used to automatically control the operation of the sampler. The transistorized relay control is further described in Appendix E.

In the main channel of the simulated servo system, amplifier 11 had two possible configurations to provide a type 1 or type 2 system. For the type 2 system, amplifier 11 was set up with the feedback resistor and the feedback capacitor in series as shown in Fig. A-1 and Fig. A-2.

The transfer function of stage 11 is then

$$\frac{e_o}{e_i}(s) = K_1 \frac{s + a}{s}$$





and the transfer function of the simulated servo is

$$G(s) = \frac{K(s + a)}{s^2}$$

where  $a = \frac{20}{R_f C_f}$  with the 20:1 time scaling included.

For the type 1 servo system, amplifier 11 was set up with the feedback resistor and feedback capacitor in parallel as shown in Fig. A-3. The transfer function for stage 11 is then:

$$\frac{e_o}{e_i}(s) = -K_1 \frac{1}{s + b}$$

and the transfer function of the simulated servo is:

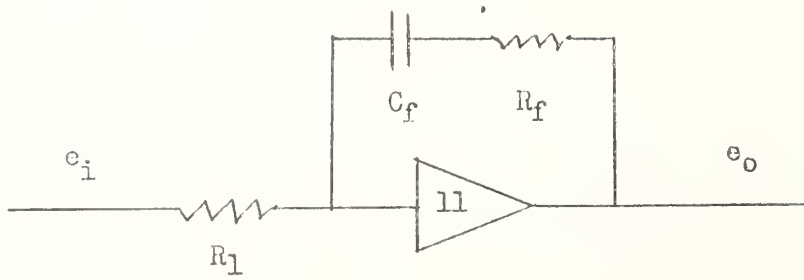
$$G(s) = \frac{K}{s(s + b)}$$

where  $b = \frac{20}{R_f C_f}$  with time scaling included.

Amplifier 10 is a sign changer necessitated by the sign change occurring in the sampler and hold stage, amplifier 9. If it is desired to simulate the servo as a continuous system without the sampler and hold for comparison of the responses in the continuous and sampled data modes of operation, amplifiers 9 and 10 can be removed from the circuit and the output of amplifier 8 connected directly to the input of amplifier 11.

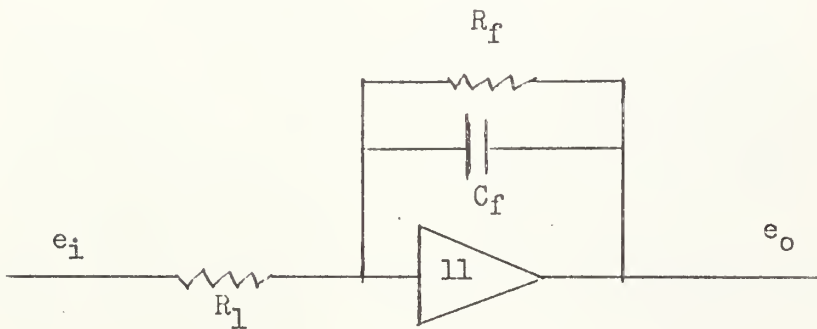
A fixed sampling frequency or manually adjustable frequency sampled data system may be simulated by connecting the output of a low frequency oscillator to the relay control circuit or, if the variable frequency oscillator has been set up, it may be used in the following manner. Disconnect





$$\frac{e_o}{e_i}(s) = -\frac{R_f}{R_1} \frac{\left(s + \frac{1}{R_f C_f}\right)}{s}$$

Fig. A-2. Stage 11 for Type 2 System.



$$\frac{e_o}{e_i}(s) = -\frac{1}{R_1 C_f} \frac{1}{\left(s + \frac{1}{R_f C_f}\right)}$$

Fig. A-3. Stage 11 for Type 1 System.



the differentiating amplifier number 1 and insert a fixed or adjustable voltage at the input of amplifier 2 or, alternatively, directly to the diode circuit of amplifier 4. The variable frequency oscillator will now operate as a conventional fixed frequency oscillator and the operation of the sampled data system with fixed sampling frequency may be observed.

The analog computer used was the Donner Model 3000 which has ten operational amplifiers. The remainder of the necessary amplifiers were, at various times in the study, Philbrick Model USA-3, GAP/R Model K2, and Boeing models, all chopper stabilized. It was found necessary to use one of the chopper stabilized amplifiers for the sampler and zero-order hold simulator, amplifier 9, since the Donner amplifiers would not respond equally to positive and negative steps under the stringent conditions imposed by the relay circuit.

Auxiliary voltages were taken from the Donner Computer initial condition board for low power uses, such as comparator levels, and from auxiliary dry cells for higher power uses, such as the relay power supply. A Hewlett-Packard Model 712 or two Model 711 power supplies were used to power the chopper stabilized amplifiers.

The analog simulation circuits used in this study have proven to be quite flexible and readily adaptable to various control arrangements. To the knowledge of the authors, this is the first analog simulation of a sampled data servo system possessing automatic sampling frequency control.



## APPENDIX B

### SAMPLER AND ZERO-ORDER HOLD SIMULATOR

The sampler and zero-order hold simulator consists of a high gain operational amplifier, a two position relay, a pair of storage capacitors which can be adjusted to an exact 2:1 ratio, and an adjustable potentiometer. The circuit is shown in Fig. B-1. Referring to Fig. 1.1, potentiometer R should be adjusted with the wiper-arm at the mid-resistance point so that,  $R_1 = R_f = \frac{R}{2}$ .

Storage capacitor  $C_1$ , between the relay arm and ground, is twice as large as feedback capacitor  $C_f$ , i.e.,

$$C_f = C$$

$$C_1 = 2C_f = 2C$$

The two relationships  $R_1 = R_f$  and  $C_1 = 2C_f$  are essential to the proper operation of the circuit. On the other hand, the exact magnitudes of R and C are not critical. (With the Boeing and Philbrick operational amplifiers in the circuit,  $R = 50K$  and  $C = 0.005 \mu f$  were found to be satisfactory.) Therefore, rather than requiring high tolerance components, the circuit was designed so that  $R_1$ ,  $R_f$ , and  $C_f$  could be adjusted with the circuit in operation, allowing the use of inexpensive components.

A small damping resistor,  $r_d$  (390 ohms), is incorporated in the feedback capacitor circuit to suppress unwanted high frequency oscillations when the relay switches. It is not





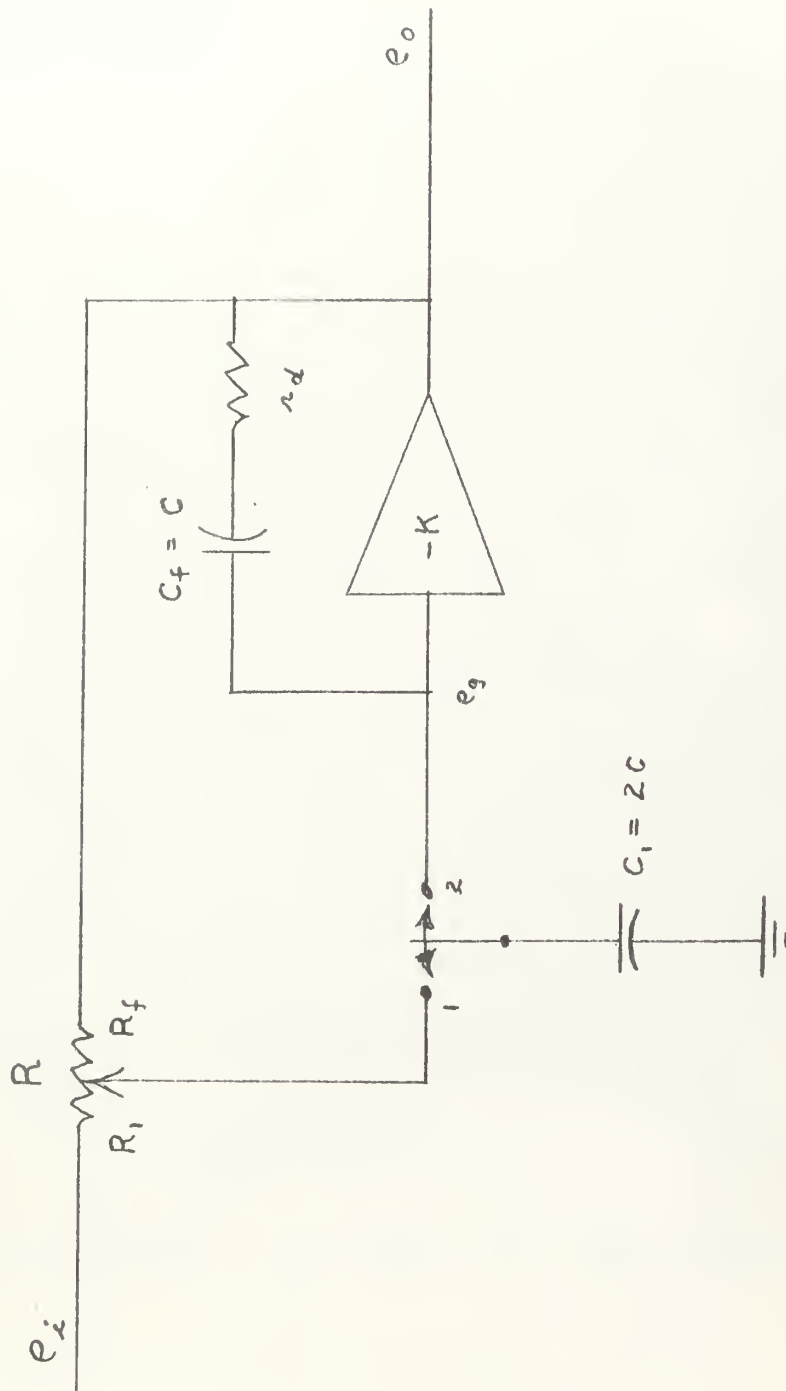


Fig. B-1. Sampler and Zero-Order Hold Simulator.



essential to the theory of operation and will be omitted from the remainder of the figures and discussion.

The sample occurs when the relay arm moves from position 1, the input side to position 2, the grid of the operational amplifier. Each time the arm moves from 1 to 2,  $e_o$  jumps to a value  $-e_i$  and holds that value until the next time the arm moves from 1 to 2. The reverse movement of the arm from 2 to 1 has no effect on  $e_o$  or  $e_i$  and can occur at any time between samples. Therefore, if the relay to be used in the circuit operates faster or more reliably in one direction than in the other, it should be installed so that the best operation is from position 1 to position 2.

A detailed explanation of the operation is as follows: Assume that the arm of the relay is to the left at position 1, the input side, and at time  $t = 0$  moves to the right to position 2, the grid side. (See Fig. B-2). Before the relay moves, at  $t = 0^-$ , the voltage across capacitor  $C_1$  is

$\frac{e_i + e_o}{2}$  since  $R_1 = R_f$  and the charge on  $C_1$  is

$$Q_1 = (2C) \frac{e_i + e_o}{2} = C(e_i + e_o) \quad (1)$$

The operational amplifier has a gain  $-K$  which should be very high, say  $10^4$  to  $10^6$ .

Then, along the forward amplifier circuit

$$e_o = -Ke_g \quad (2)$$

Around the feedback circuit

$$e_g = e_o + \frac{Q_f}{C_f} \quad (3)$$



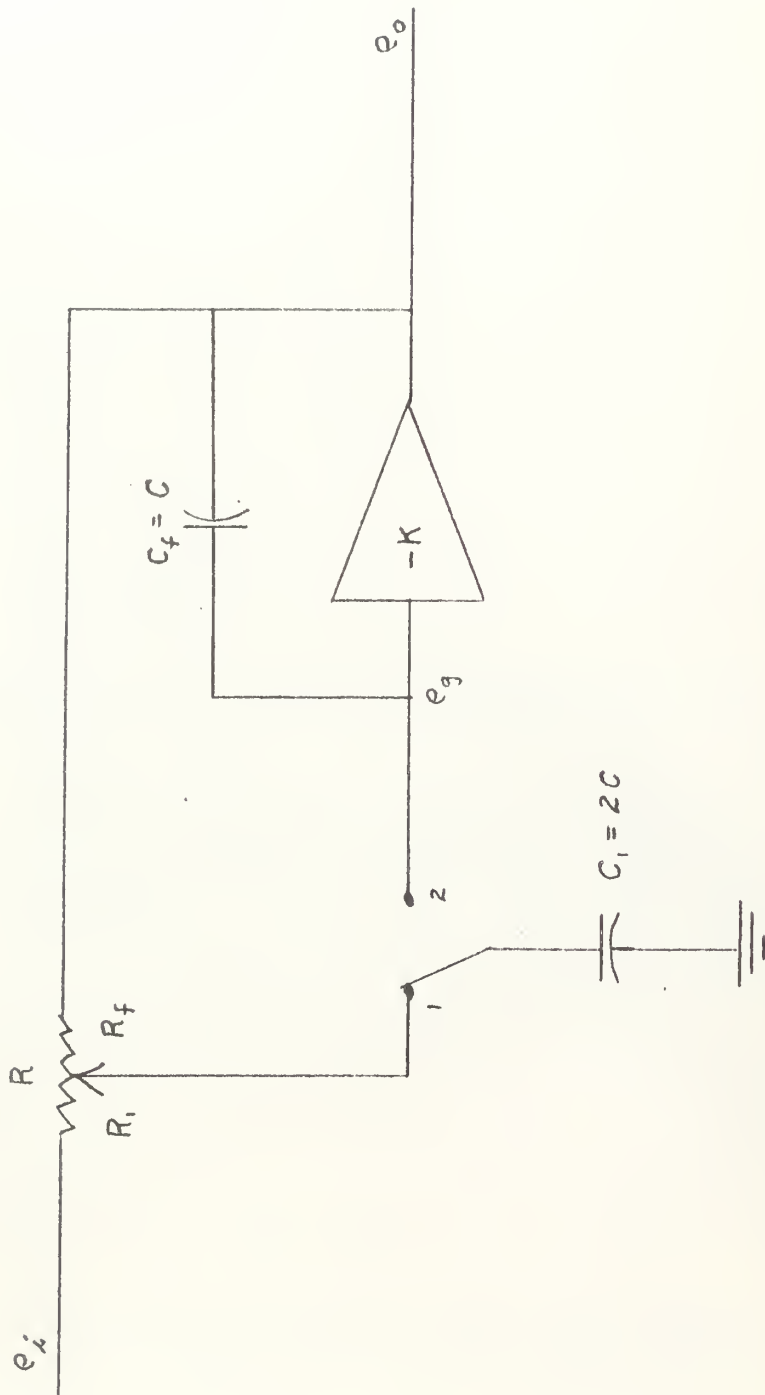


Fig. B-2. Sampler and Zero-Order Hold. Instant before sample time.



Combining (2) and (3)

$$e_o = -Ke_g = -K\left(e_o + \frac{Q_f}{C_f}\right) \quad (4)$$

Rearranging:

$$e_o = \frac{-K \frac{Q_f}{C_f}}{1 + K} \quad (5)$$

But since  $K \gg 1$ ,

$$e_o \approx -\frac{Q_f}{C_f} \quad (6)$$

Then, by (3) and (6)

$$e_g = -\frac{Q_f}{C_f} + \frac{Q_f}{C_f} = 0 \quad (7)$$

From (6) the charge on the feedback capacitor  $C_f$  is

$$Q_f = -C_f e_o = -C e_o \quad (8)$$

At  $t = 0$  the relay arm moves to position 2, the grid of the operational amplifier. (Fig. B-3). The total charge on the grid circuit is now the sum of the separate charges on the two capacitors before the switch:

$$Q = Q_1 + Q_f \quad (9)$$

Then, from (1) and (8)

$$Q = C(e_i + e_o) - C e_o = C e_i \quad (10)$$

Around the operational amplifier the same relations still hold between  $e_g$  and  $e_o$ ; hence, the final result must be that  $e_g = 0$ . The only way for this requirement to be met is for capacitor  $C_1$  to be discharged, the entire





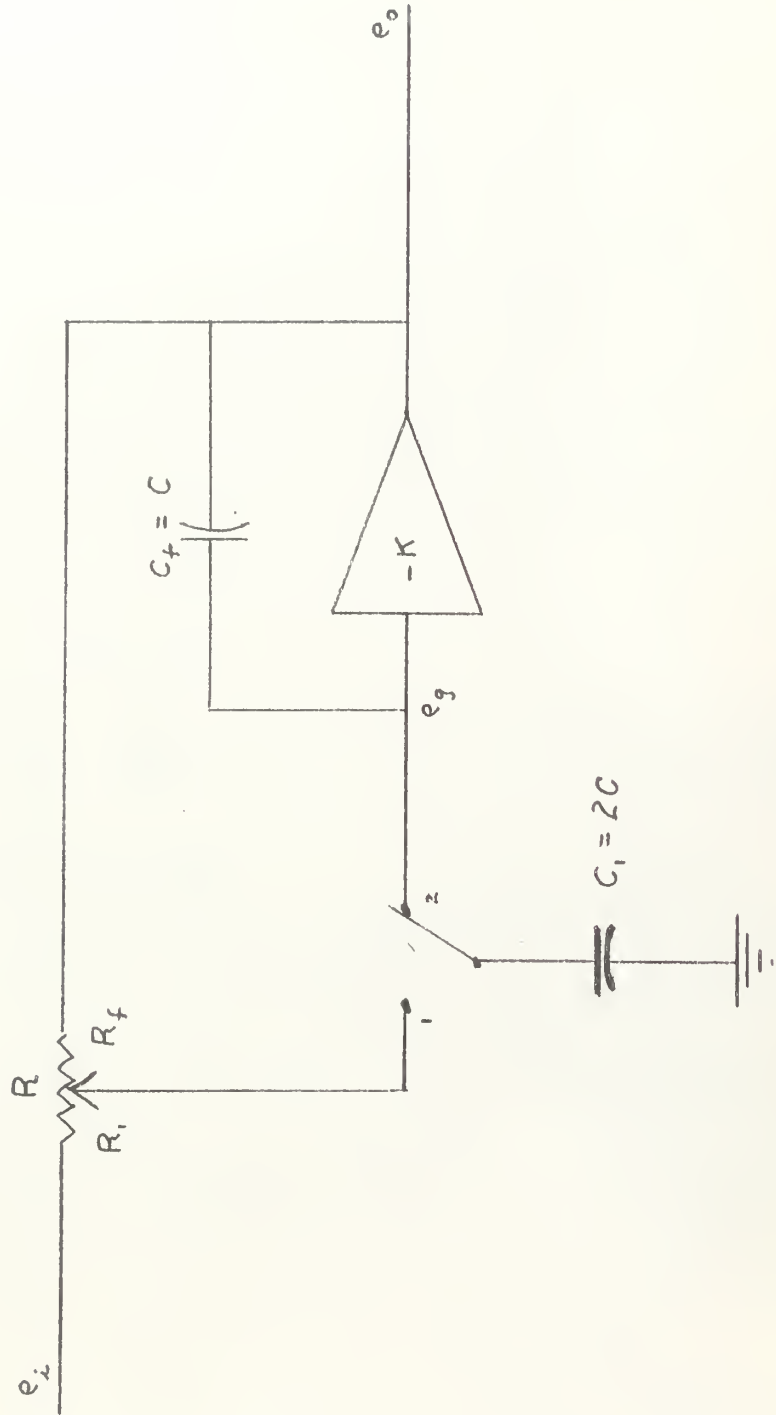


Fig. B-3. Sampler and Zero-Order Hold. Instant after sample time.



charge going to feedback capacitor  $C_f$  . That this is true physically can be seen by the following analysis: Assume that  $\frac{e_i + e_o}{2}$  is positive. Then, at the sample time, a positive voltage is suddenly applied to the grid circuit of the operational amplifier driving the output negative. Because of the high gain of the amplifier, the output continues increasing negatively until the grid voltage is reduced to zero via the feedback capacitor  $C_f$  . Then the charge on capacitor  $C_1$  is zero and the charge on  $C_f$  becomes, from equation (10):

$$Q_{f2} = Q = Ce_i \quad (11)$$

Then, from equation (6):

$$e_o = \frac{-Q}{C_f} = \frac{-Ce_i}{C} = -e_i \quad (12)$$

which is the desired result.

Thus,  $e_o$  jumps from its original value to  $-e_i$  at  $t = 0$  . The feedback capacitor holds  $e_o$  constant until the relay arm moves back to the input side and then returns to the grid with another charge  $Q$  . The circuit thereby accomplishes its purpose; namely, to sample the input when the switch is operated, reproduce the input magnitude at its output, and hold the magnitude constant between sample times.

If there is any delay between the time the relay leaves side 1 and the time it arrives at side 2, there will be an equal delay in the sampled output. The speed of the return movement is not critical and can occur at any time between samples. The relay used in this study was a Potter and



Brumfield Model SC11D. At the sampling frequencies used there was no significant delay time arising from the relay operation.

For proper operation of the circuit, the potentiometer R must be adjusted so that the voltage at position 1 is exactly the average of the input and output voltages, i.e.,

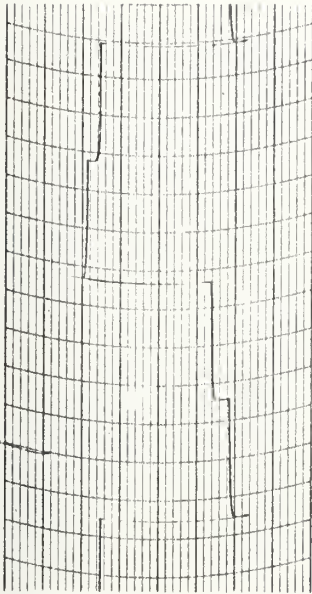
$$e_1 = \frac{e_i + e_o}{2}$$

Also, the in-circuit capacitances of  $C_1$  and  $C_f$  must be in an exact 2:1 ratio. In order to meet these requirements, it was found necessary to calibrate or adjust the system after construction. Calibration procedure is as follows:

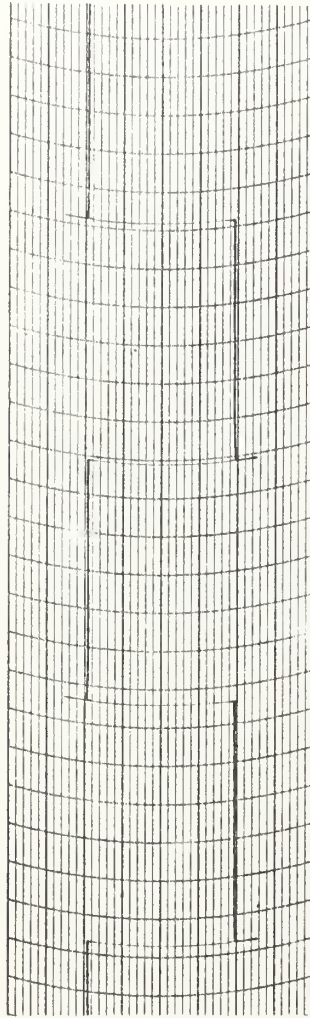
Use a square wave from a low-frequency function generator for a test input. Operate the sampler at a frequency at least four times that of the test input so that at least two output samples can be observed during each half-cycle of the test input. If the circuit is not properly adjusted, the output will overshoot or undershoot on the first sample of each half-cycle of the input. (Fig. B-4a). After proper adjustment of the potentiometer and the capacitance, the output will be a rectangular wave of the same amplitudes as the input with a time delay less than or equal to the sample period. (Fig. B-4c). Note that in Fig. B-4a the sampling frequency is approximately four times the square-wave input frequency and in Fig. B-4c the sampling frequency is about ten times the test input frequency; however, the overshoot or undershoot is dependent only on the adjustment of the circuit, not on the



(a) Typical uncalibrated response.



(b) Input.



(c) Calibrated output.

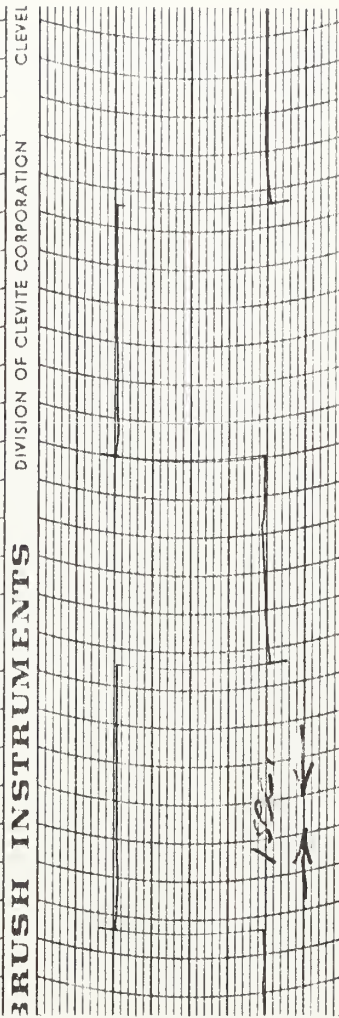


Fig. B-4. Sampler and Zero-Order Hold. Response to step inputs showing effect of calibration.





relative frequencies. If both the potentiometer and the capacitances are miscalibrated, it is possible for the overshoot or undershoot condition not to appear, but the output voltage will not have the same magnitude as the input. Both the potentiometer and the trimmer capacitors must be adjusted simultaneously to attain the calibrated condition of no undershoot or overshoot and exact equality of output to input. Recordings of the sampled output of a triangular input function are shown in Fig. B-5 over a range of sampling frequencies.

It should be noted that the only requirement on the relay for accurate sampling results with this circuit is the absence of switching delay time in one direction, a requirement which can be readily met by commercially available relays. This two capacitor sampler and hold also has zero pulse width since the instantaneous input at the switching time is held as a constant output until the next sample time. By way of contrast, the usual type of single capacitor sampler and hold, shown below, requires the relay to close and open rapidly for a narrow but finite pulse width. Also, capacitor  $C_f$  must be large enough to hold the output constant between samples but time constant  $R_1 C_f$  must be small compared with the pulse width in order for the output to reproduce the input magnitude.

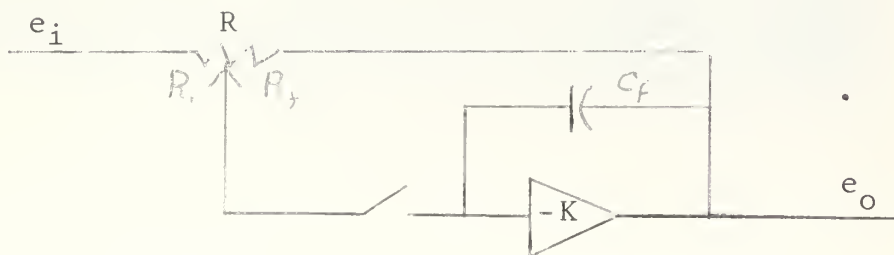


Figure B-6. Ordinary One-Capacitor Hold.



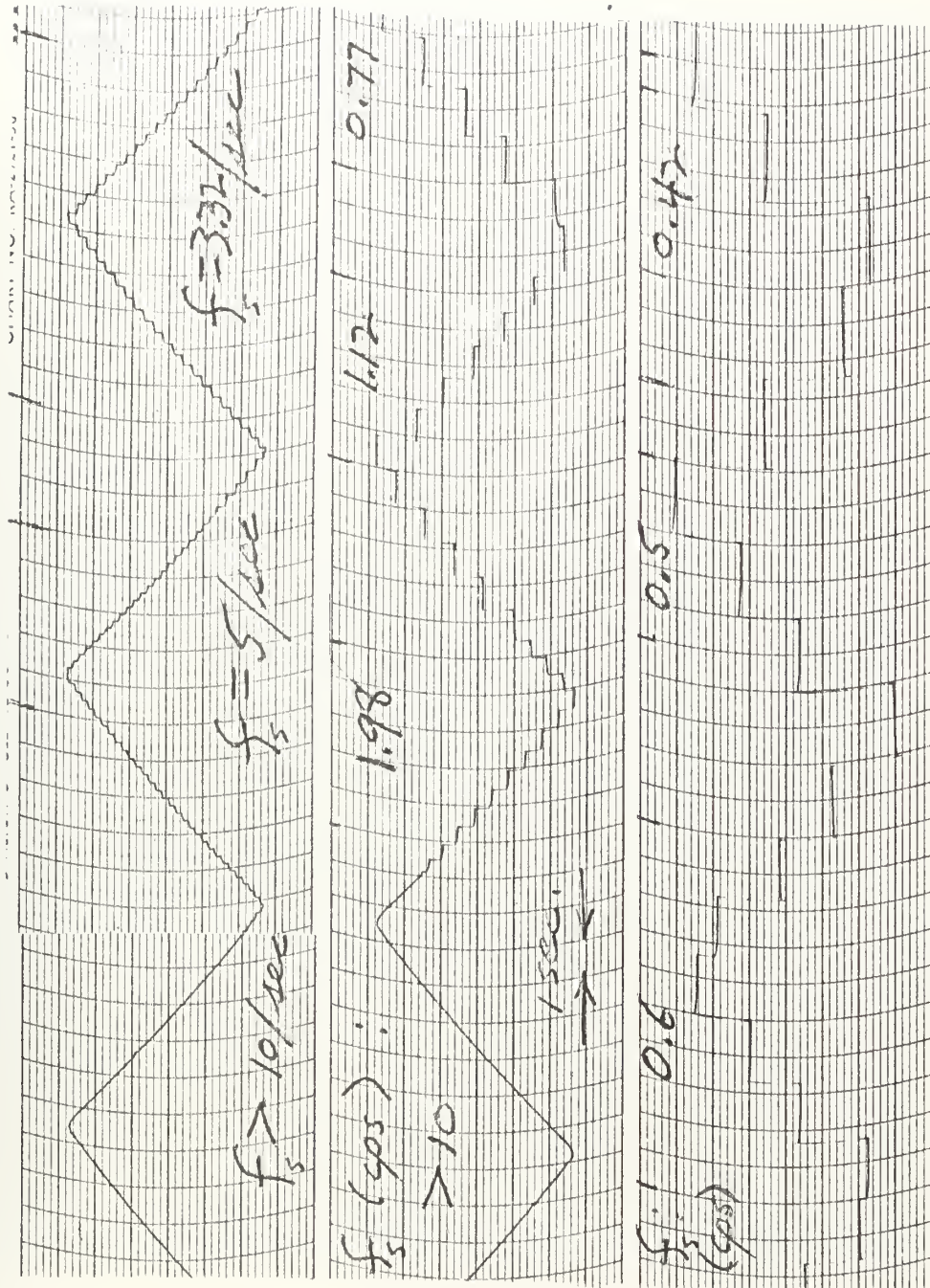


Fig. B-5. Sampler and Zero-Order Hold. Response to ramp inputs at various sampling frequencies.



It was felt that the two capacitor circuit used here was very successful and several circuits were constructed as plug-in units.



## APPENDIX C

### DIFFERENTIATOR AND ABSOLUTE VALUE DETECTOR CIRCUITS

The conversion of the error signal  $E$  to a signal which is a function of the time derivative of  $E$  is accomplished in two analog simulated circuits. These circuits are shown in Fig. C-1. The two circuits are a differentiating circuit and a precision absolute value detector with limiting.

The differentiating circuit is accomplished in a conventional manner using one high gain amplifier. In Fig. C-1 the differentiating circuit uses amplifier 1. Adequate response and stability were achieved by employing a 15 K damping resistor in the input to the ordinarily noisy analog differentiator circuit. It is to be noted here that the differentiator serves its purpose adequately by providing relative rates rather than by being required to provide absolute derivative values for successful control signal generation. The input to the differentiating stage is  $\pm E$  and the output, which may be scaled as desired, is in this case  $\pm \dot{E}$ .

The second stage of the conversion is the absolute value detector circuit. Fig. C-1 shows amplifiers 2 and 3 with the circuitry for the absolute value detector. This circuit was designed by modifying a precision absolute-value device (linear full-wave rectifier) circuit suggested by Korn and Korn<sup>7</sup> and Morrill and Baum<sup>6</sup>. If the feedback circuit for amplifier 3 consists only of the 2 Megohm resistor, the absolute value





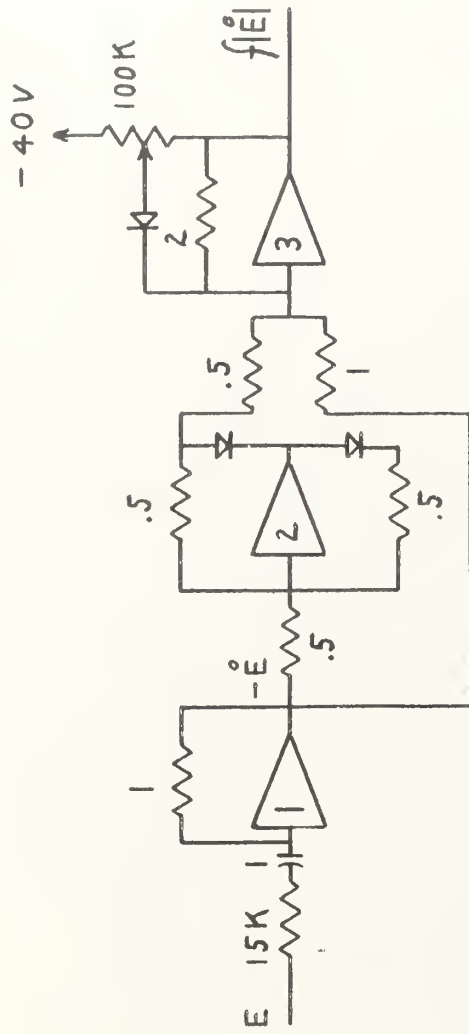


Figure C-1-1. Differentiator and absolute value detector circuit.



detector output is as shown in Fig. C-2a. However, the desired control output was achieved by employing diode limiting in the feedback path of amplifier 3. This resulted in the output as shown in Fig. C-2b. In Fig. C-1 it is seen that once the upper feedback diode of amplifier 2 begins to cut off, the high amplifier gain of amplifier 2 limits the output sharply. The lower feedback diode of amplifier 2 prevents amplifier overloads when the input signal to amplifier 2 goes negative. Morrill and Baum have shown that the voltage feedback arrangement leaves the circuit gain essentially independent of the diode plate resistance and thus the output follows the input quite precisely. (See Fig. C-3). The absolute value detector separates the magnitude from the sign of an input signal by a signal discriminating process. All input signals are either positive or negative. If the input signal is  $+x_1$ , amplifier 2 acts as a 1-to-1 sign changer and changes the signal from  $+x_1$  to  $-x_1$  and amplifier 3, a scaled summer, then adds  $-4x_1$  and  $+2x_1$  and changes the sign of the summation so that  $-((-4x_1 + (+) 2x_1)) = +2x_1$  is the output of the  $+x_1$  input. If the input signal is  $-x_1$ , then amplifier 2 has 0 output and amplifier 3 adds 0 and  $-2x_1$  changing the sign of the summation so that  $-(0 + (-) 2x_1) = +2x_1$  is the output of the  $-x_1$  input. Thus  $x_0 = 2|x_1|$ . (See Fig. C-1 for graphic representation.) If necessary,  $x_0 = -2|x_1|$  is achieved by reversing the diodes and bias voltages. The output magnitude may be scaled as desired by varying the feedback



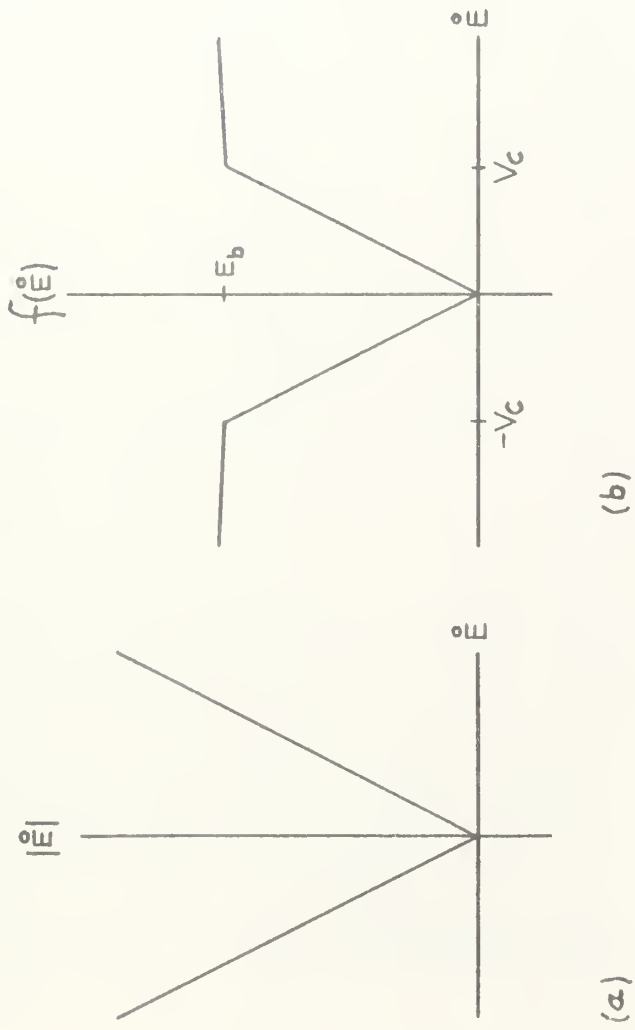
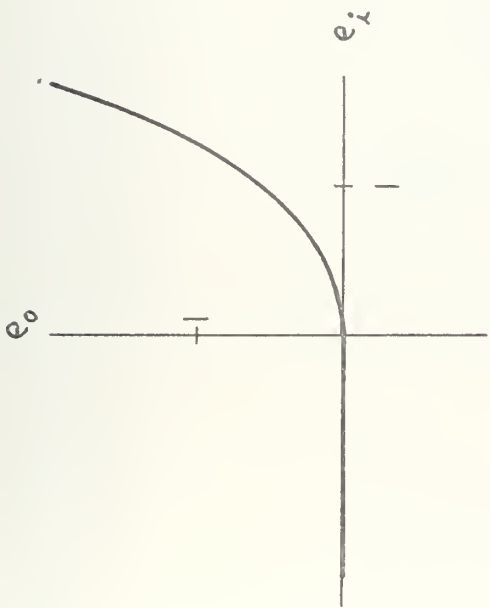
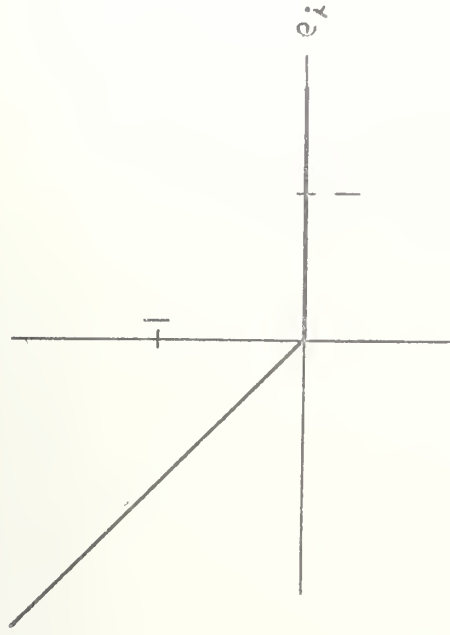


Figure C-2. Absolute value detector output:  
 (a) without limiting, and  
 (b) with limiting.





$$i_d = I_0 e^{\alpha(e_i - e_0)}$$



$$i_d = I_0 e^{\alpha K(e_i + e_0)}$$

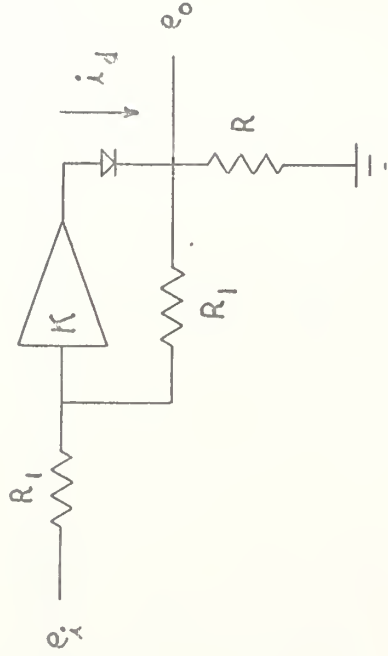
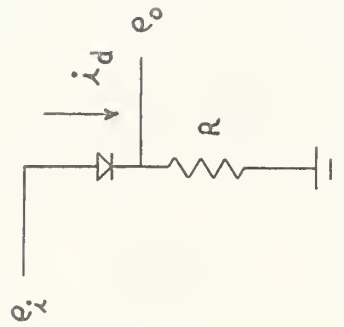


Figure C-3. Circuit for achieving ideal diode characteristics with high gain amplifier.





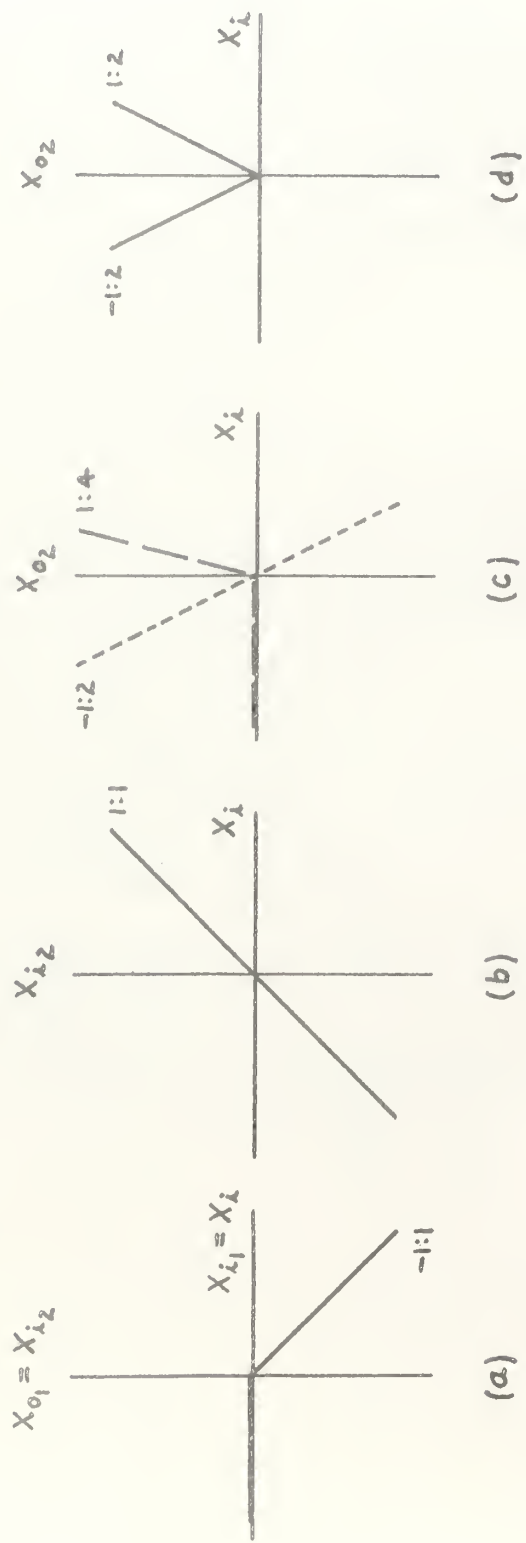


Figure C-4. Graphical illustration of absolute value detection process: (a) output of amplifier 2, (b) input to amplifiers 2 and 3, (c) components of output of amplifier 3, (d) output of amplifier 3.



resistor value in amplifier 3. If the feedback resistor used has the value  $kR_1$ , then the output is  $x_o = k |x_i|$ . The output of the absolute value detector can be DC biased as desired. The diode limiter in the feedback path of amplifier 3 changes the slope of the output after the break voltage. Absolute value detection with limiting then allows monotonic function generation with the input the independent variable. In this case, a simple function

$$x_o \begin{cases} = k_1 |x_i| & (-V_c \leq x_i \leq V_c) \\ = k_2 |x_i| + V_c(k_1 - k_2) & (|V_c| \leq x_i) \end{cases}$$

was adequate for the desired signal generation. The slopes  $k_1$  and  $k_2$  are determined by the feedback resistances, and the break points,  $V_c$ , are determined by the diode biasing voltages. Fig. C-5 shows the relationship of the feedback limiter to the output as used in amplifier 3. The slope of the diode limited branch ( $x_o > E_b$ ) is

$$= \frac{R_f (r_b + r_d)}{R_1 (R_f + r_b + r_d)}$$

where  $r_d$  is the diode resistance and the slope of the unlimited branch ( $x_o < E_b$ ) is  $-\frac{R_f}{R_1}$ . Thus, as  $r_b$  and  $r_d$  become very small with respect to  $R_f$  and  $R_1$ , the slope of the diode limited branch approaches  $-\frac{1}{R_1}$ .

A desired sampling time control relationship is  $T = \frac{c_1}{\sqrt{|E|}}$



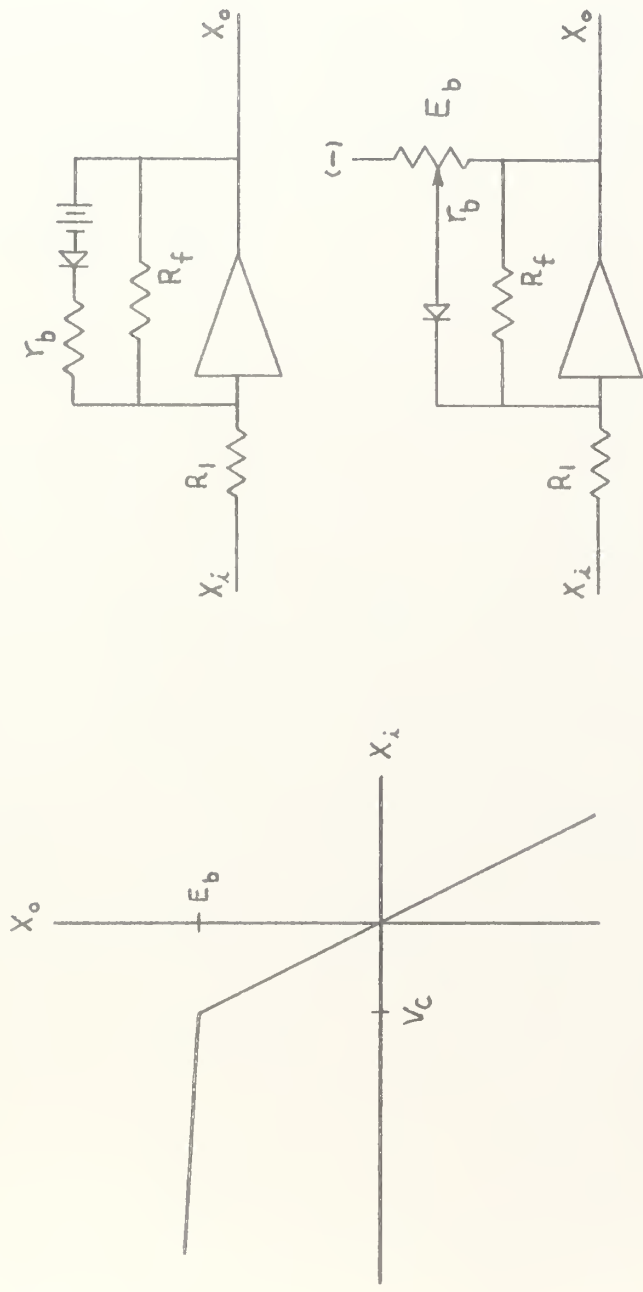


Figure C-5. Feedback limiter circuit.



where  $c_1$  is a constant.  $T = \frac{1}{f_s} = \frac{c_1}{\sqrt{|\dot{E}|}}$  so  $c_1 f_s = \sqrt{|\dot{E}|}$  or  
 $c_2 f_s^2 = |\dot{E}|$  where  $c_2$  is a constant and  $f_s$  is the sampling  
 frequency, is a desired response of the voltage controlled  
 oscillator to the controlling  $|\dot{E}|$  input. Therefore, the  
 diode limited branch of the absolute value detector was adjusted  
 to produce an output of the voltage controlled, variable  
 frequency oscillator which approximated the desired test  
 function of  $c_2 f_s^2 = |\dot{E}|$ .





## APPENDIX D

### THE VOLTAGE CONTROLLED OSCILLATOR

The voltage controlled variable frequency oscillator is simulated on the analog computer by a free-running multi-vibrator which has a period controlled by a voltage input. The circuit is an extension of a fixed period astable multi-vibrator described by Morrill and Baum (Ref. 6). It consists of four amplifier stages: two comparators, an integrator, and a sign changer. The arrangement is shown in Fig. D-1. The control voltage  $|\dot{E}|$  is applied through a 45-volt bias battery to one of the diode circuits on comparator amplifier 4. The output of comparator amplifier 5 is then a square wave of constant amplitude having a period  $T$  governed by the equation  $T = A(45v - |\dot{E}|)$  sec. It is this output voltage which is used to control the sampler circuit in the simulated servo system. An explanation of the circuit operation and derivation of the equation for  $T$  follows.

Amplifiers 4 and 5 are comparators. Their operation will be explained with the aid of Fig. D-2. In Fig. D-2a,  $R_1$  and  $R_2$  are much larger than  $r_1, r_1', r_2, r_2'$ . In this project,  $R_1$  and  $R_2$  were 1 megohm and  $r_1 + r_1', r_2 + r_2'$  were 25K ohms. The diodes used were GE 1N538 silicon-junction rectifiers.

The relationship between the grid voltage  $e_g$  and the output voltage  $e_o$  is, along the amplifier forward path,

$$e_o = -Ke_g . \quad (1)$$



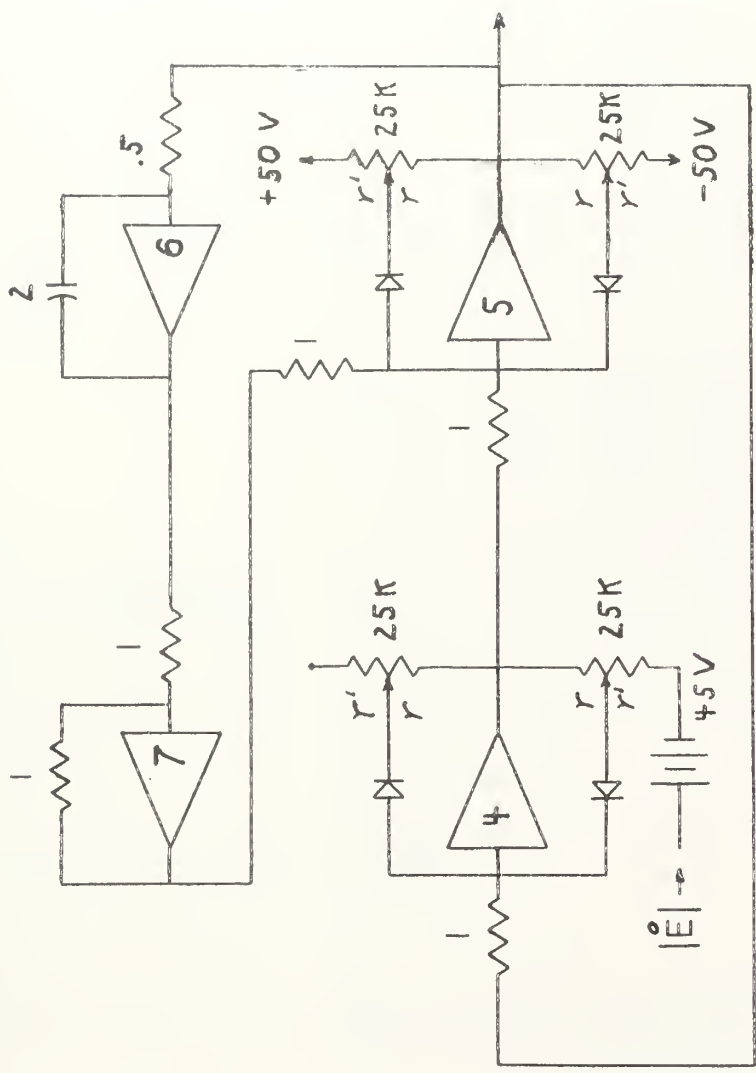
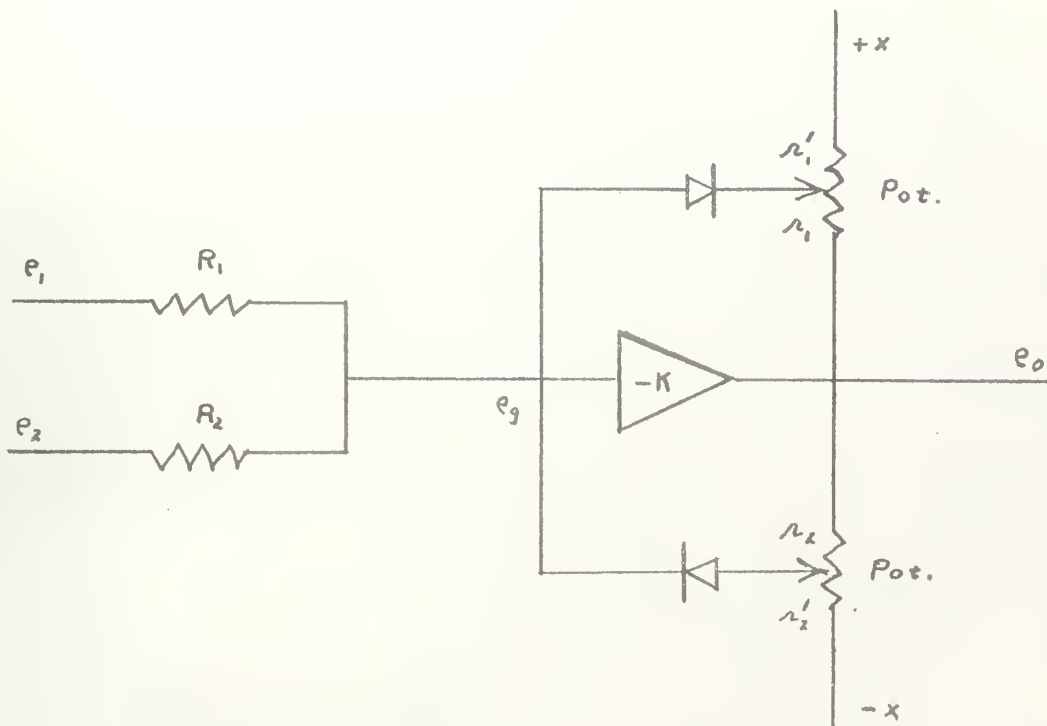
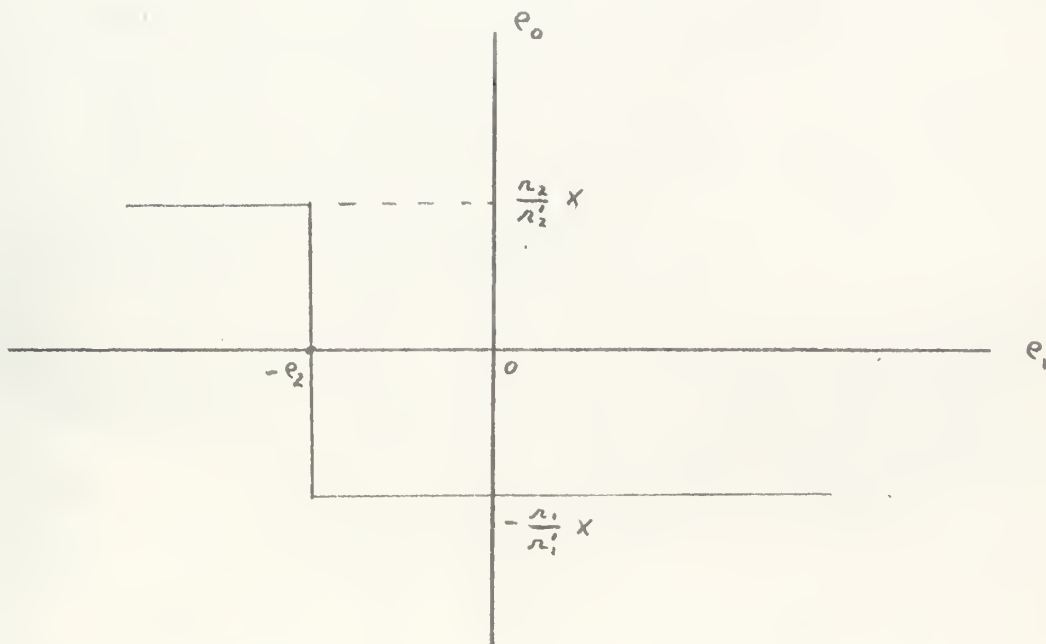


Figure D-1. Voltage controlled oscillator circuit.





(a) Circuit.



(b) Output.

Fig. D-2. Comparator.



To find the relationships around the feedback paths, assume that a small positive voltage is applied to the grid. Then  $e_o$  is negative and the lower feedback path is certainly cut off. The upper diode is cut off if the voltage at the potentiometer arm is more positive than  $e_g$ . In that case, the gain of the stage is  $-K$  since both feedback loops are open circuit. Since  $K$  is very large in the operational amplifier,  $e_o$  decreases until the voltage at the potentiometer arm is less than the grid voltage. Then the upper diode conducts and, assuming negligible forward resistance in the diode, the gain of the stage becomes practically zero since  $r_1 \ll R_1$  and the gain of an operational amplifier with resistive feedback is  $\frac{r_1}{R_1} \ll 1$ . The relationship between the grid voltage and the output voltage around the feedback path is

$$e_g = e_o + ir_1 \quad (2)$$

$$\text{Combining (1) and (2),} \quad e_o = -K(e_o + ir_1) \quad (3)$$

$$\text{Rearranging:} \quad e_o = \frac{-ir_1}{1 + K} \cong -i r_1 \quad (4)$$

since  $K \gg 1$ .

$$\text{Then from (2)} \quad e_g = e_o + ir_1 \cong -ir_1 + ir_1 = 0 \quad (5)$$

Thus, the voltage on the potentiometer arm for the diode to just conduct is approximately zero.

Since  $R_1$ ,  $R_2$  are much greater than  $r_1$ ,  $r_1'$  the current flowing from the input voltage sources will be negligible compared with the current from the clamping voltage source  $+X$ . Then the current through the entire potentiometer





$$\text{is } i = \frac{X}{r_1} = -\frac{e_o}{r_1} \quad (6)$$

Thus, the output is clamped to

$$e_o = -X \frac{r_1}{r_1} \quad (7)$$

Likewise, if a small negative voltage is on the grid, the output voltage will be

$$e_o = -(-X \frac{r_2}{r_2}) = X \frac{r_2}{r_2} \quad (8)$$

since the lower feedback diode will be in operation.

The division point for the output to switch from one voltage to the other is the zero potential point of the grid circuit, or the point at which the sum of the input voltage is zero. Thus, the output switches from one polarity to the other when  $e_1 + e_2 = 0$ , that is when  $e_1 = -e_2$  as shown in Fig. D-2b.

Referring again to Fig. D-1, comparator amplifier 4 has only one input to the grid circuit, the output of comparator amplifier 5. The clamping voltages are  $(-45 + |\dot{E}|)$  and zero. Hence, the output of amplifier 4 will be zero when its input is positive and  $a(45 - |\dot{E}|)$  when its input is negative. Where "a" is the potentiometer setting  $\frac{r_2}{r_1}$  in the lower feedback circuit. The reason for using the control voltage  $|\dot{E}|$  in this manner will be seen in the final expression for T. Comparator amplifier 5 has two inputs from amplifiers 4 and 7 and, hence, will switch when  $e_4 + e_7 = 0$ .

The clamping voltages and potentiometers are set so that



the output will be clamped to  $\pm 50 b$ , where "b" is the potentiometer setting for both diode circuits in comparator 5, the sign used being opposite to  $e_4 + e_7$ . In practice, the two potentiometer settings were made approximately equal by screwdriver adjustment, there being no need for precise equality.

Waveforms of the outputs of the multivibrator stages are shown in Fig. D-3. Integrating amplifier 6 has a ramp output of slope

$$\pm \frac{50b}{(0.5)(2)} = \pm 50b$$

Amplifier 7 reverses the slopes of the ramps.

Whenever  $e_7 = -e_4$ , comparator 5 switches, i.e., at

$$e_7 = 0$$

and at  $e_7 = -(45v - |\dot{E}|) a$

Since  $e_7$  is a ramp of constant slope  $\pm 50b$ , the time for a half cycle can be derived from the equation

$$-50 bt = -(45 - |\dot{E}|) a$$

or

$$t = \frac{(45 - |\dot{E}|) a}{50 b}$$

and the period of a complete cycle is

$$T = \frac{(45 - |\dot{E}|) a}{25 b}$$

This equation is of the form

$$T = A(45 - |\dot{E}|)$$

and is graphed in Fig. D-4a.

As explained in Appendix C the control voltage  $|\dot{E}|$  may be shaped to provide desired frequency control characteristics.



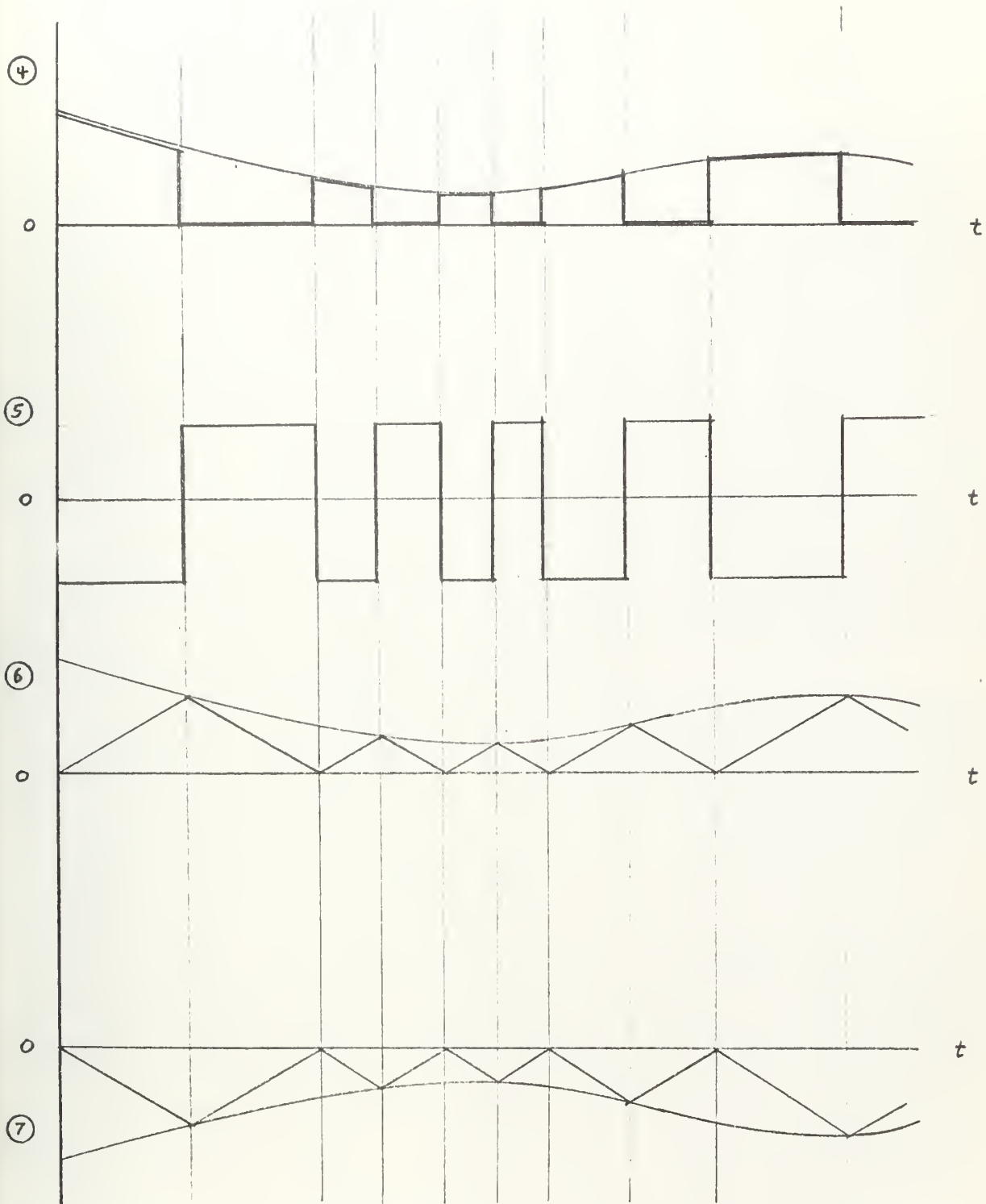


Figure D-3. Multivibrator waveforms.



In this study, one scheme used was to multiply  $|\dot{E}|$  by a constant and limit it in the absolute value detector. Fig. D-4b is a typical T vs.  $|\dot{E}|$  curve resulting from such shaping. Another method of control was to make the absolute value detector also a comparator so that two fixed control voltage levels appear as the input to the multivibrator, Fig. D-4c is the resulting two-level T vs.  $|\dot{E}|$  graph. Obviously, many more complicated functions of  $|\dot{E}|$  could be generated by extensions or combinations of these methods or by using an electronic function generator such as Donner Model 3750. Fig. D-5 shows actual recordings of the multivibrator waveforms as  $|\dot{E}|$  is varied. The T vs.  $|\dot{E}|$  characteristic for these recordings was of the type shown in Fig. D-4b.

If  $|\dot{E}|$  changes during the sampler cycle, as will often be the case, the time for one complete period beginning and ending with  $e_7 = 0$  will be set by the value of  $|\dot{E}|$  at the mid-cycle point when

$$t = \frac{A(45 - |\dot{E}|)}{2} .$$

Thus, the sampling frequency is changed once per cycle by a single value of the control voltage. If the inverse of the control voltage plus bias were applied to the second diode circuit of comparator stage 4, both the plus and minus limits of its output would vary and stage 7 would then integrate between two variable levels instead of one variable and one fixed level. The sample period would then be set by two values of  $|\dot{E}|$  per sample cycle. Future experimentation might indicate whether the added complexity of the control circuit





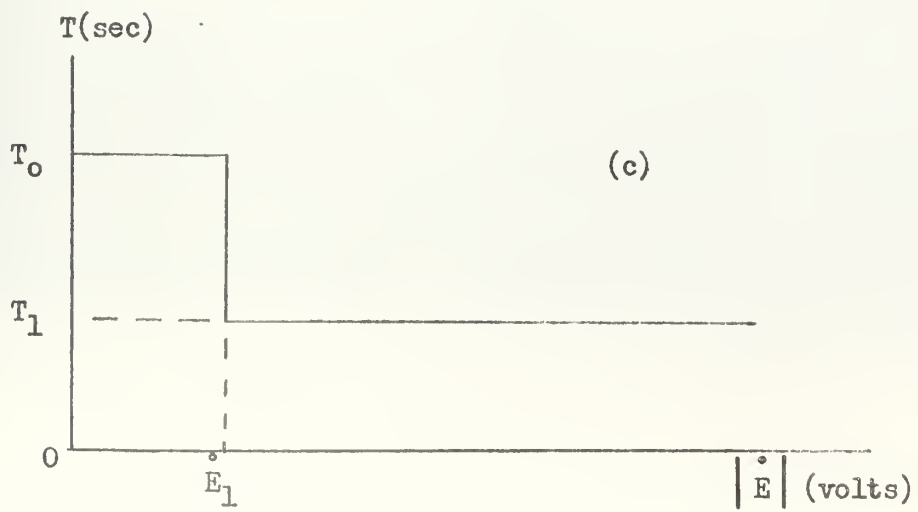
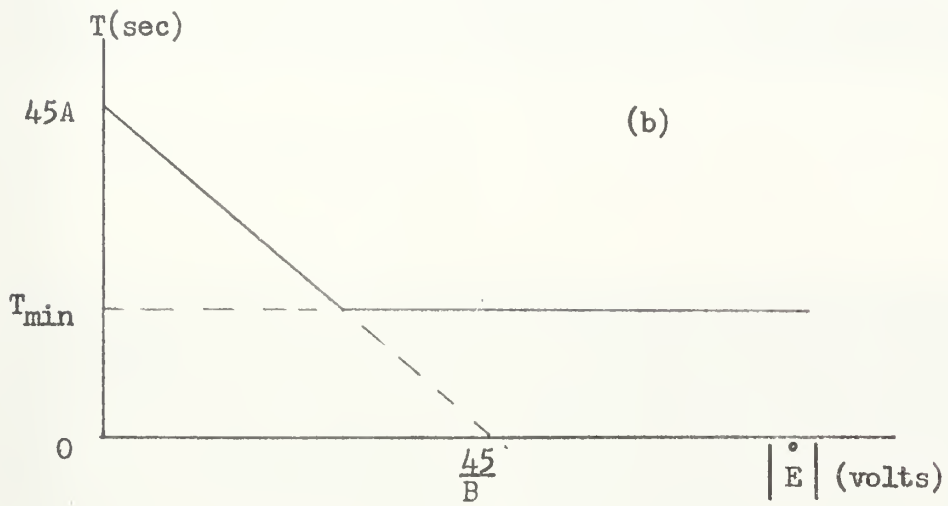
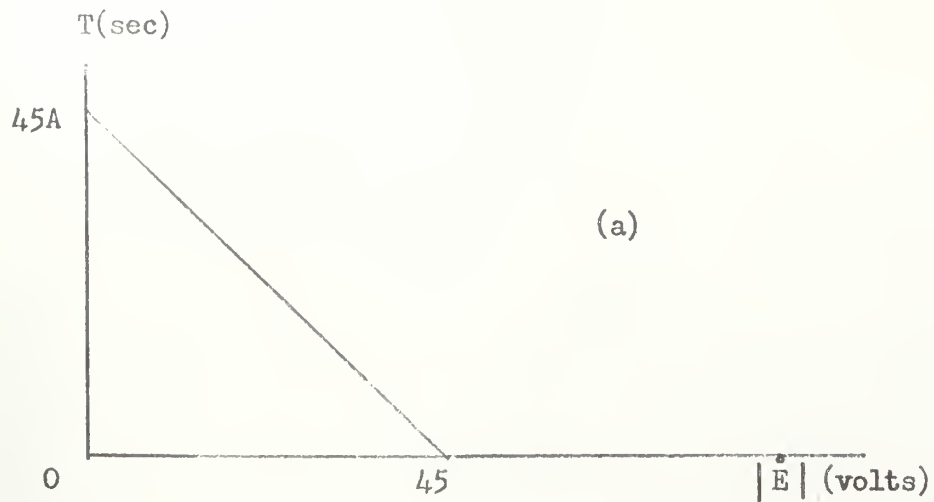
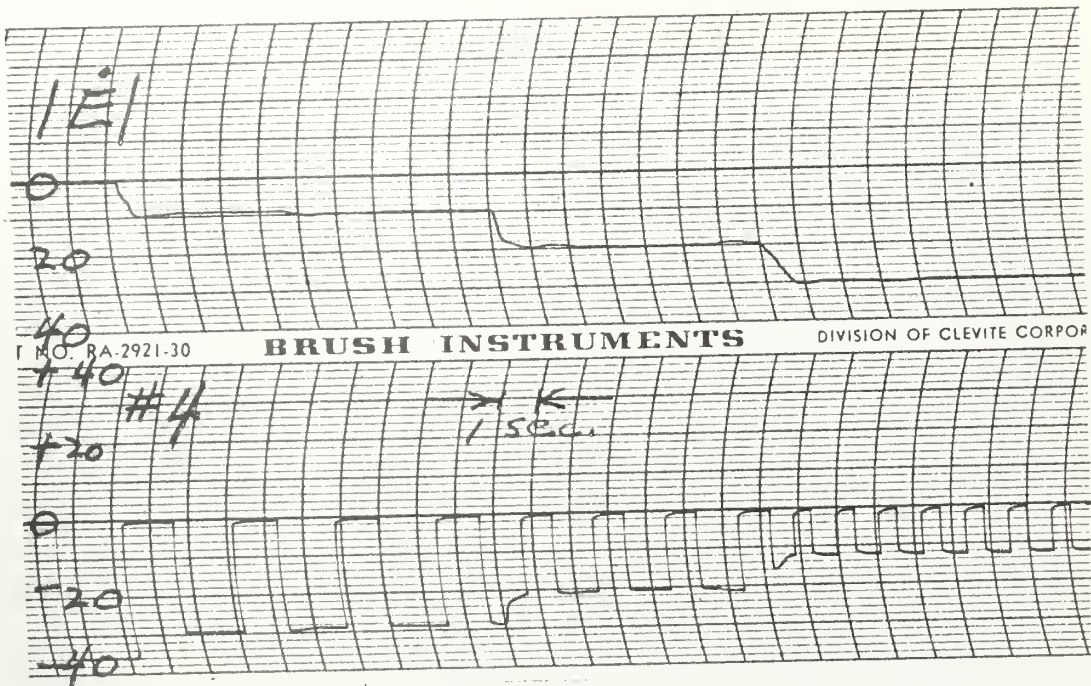
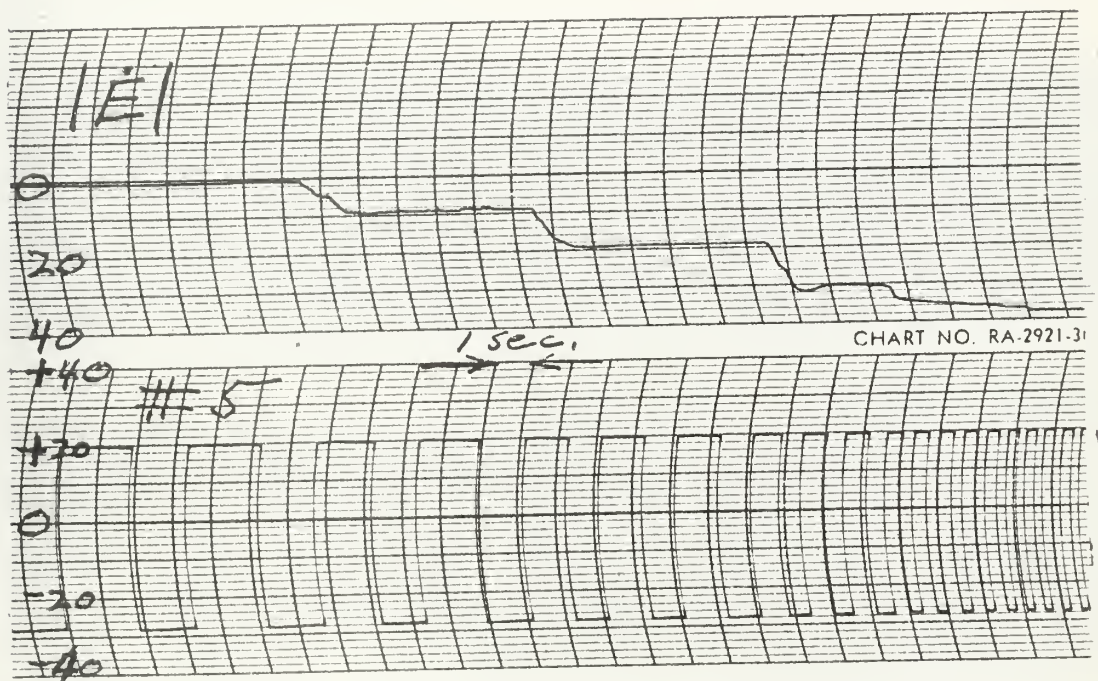


Fig. D-4. Sample Period,  $T$  vs.  $|\dot{E}|$ .





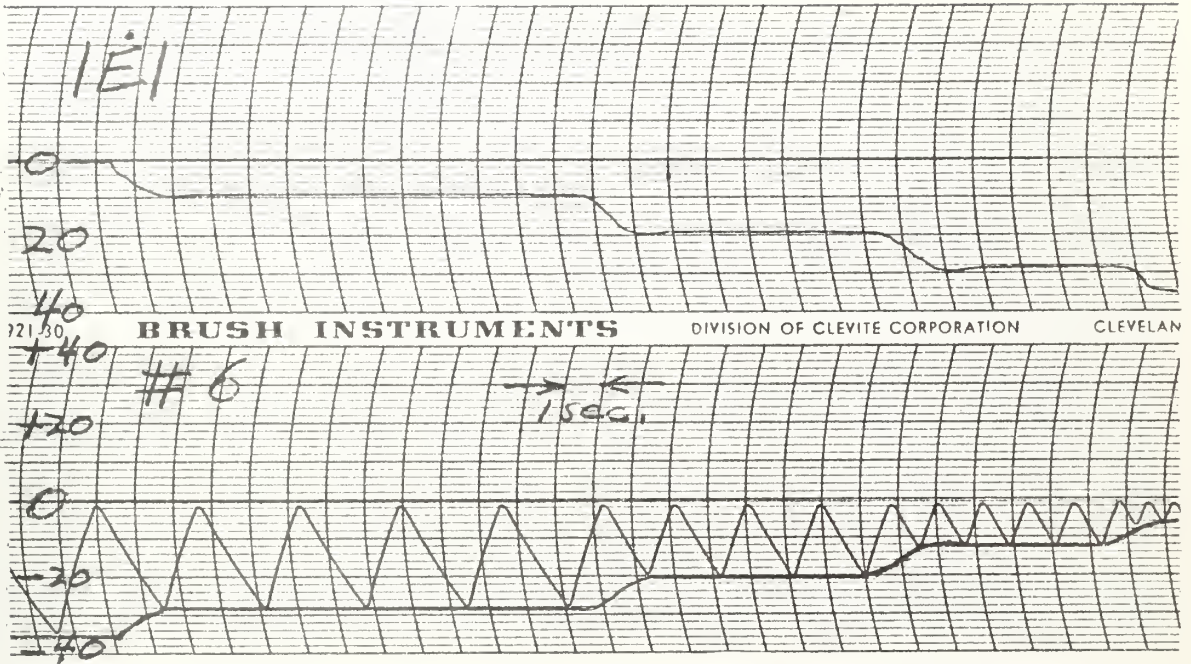
(a) Output of amplifier #4



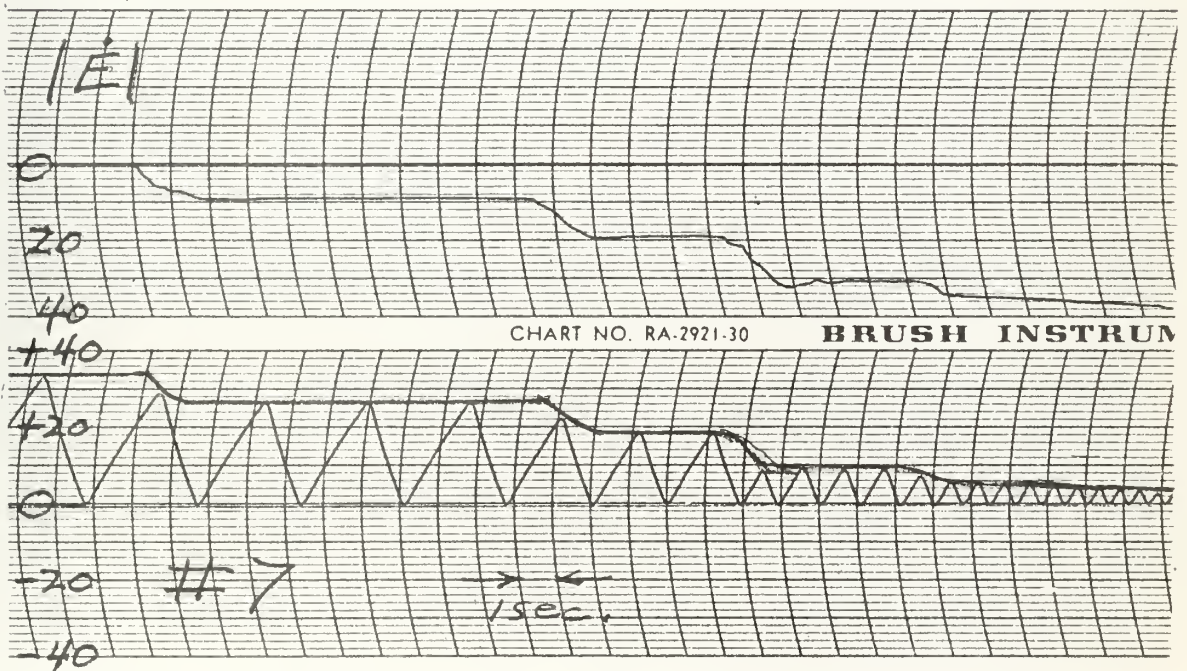
(b) Output of amplifier #5

Fig. D-5 Oscillator Waveforms





(c) Output of amplifier #6



(d) Output of amplifier #7

Fig. D-5 Oscillator Waveforms



for such a system could be justified by improved performance.

Another multivibrator control method not used in this project would be to reverse the roles of the comparators by applying  $\pm 50$  volts to the diode circuits of stage 4 and the  $|\dot{E}|$  control voltage to the diode circuits of stage 5. Then  $e_7$  always integrates to the same voltage  $\pm 50a$ , but integrator stage 7 now produces an output of slope  $\pm b |\dot{E}|$ . Then switching takes place when

$$b \int_0^t |\dot{E}| dt = 100 a$$

Thus, the period is a function of the value of  $|\dot{E}|$  integrated over the entire sample period rather than the value at one or two points in the cycle as in the two previous cases. If  $|\dot{E}|$  is constant

$$b |\dot{E}| t = b |\dot{E}| \frac{T}{2} = 100 a$$

the period,

$$T = \frac{200a}{b |\dot{E}|} = \frac{1}{C |\dot{E}|}$$

and the sampling frequency is:

$$f_s = C |\dot{E}|$$

If  $|\dot{E}|$  varies rapidly during the sample period, this period might give better control; however, the sample period would probably have to be reduced to properly control a servo whose velocity varied so rapidly. Therefore, the assumption made during this project that  $|\dot{E}|$  would not change erratically during a sample period seems valid.

If  $|\dot{E}|$  were not available as a continuous variable, but





only by computing backward differences on the sampled error signal, then any of these methods would be dependent on a single estimate of  $\dot{E}$  in each sample period. The principal reason for using the single point control in this project was that it was the simplest method available and the results were very satisfactory.



## APPENDIX E

### TRANSISTORIZED SAMPLER RELAY CONTROL

The function of sampling with a zero order hold is accomplished by the sampler and zero order hold simulator circuit. See Fig. E-1. The simulator circuit samples the error signal  $E$  and then maintains or holds this signal level  $E_h^*$  until the next sample is taken by the switching action of a two-position relay in the sampler and zero order hold simulator circuit. The switching of this relay is controlled by the output signal of the voltage controlled oscillator. The relay control circuit is shown in Fig. E-1. The circuit is composed of a Potter and Brumfield SC11D 24 V-DC two-position relay and a 2N597 transistor. The transistor is base controlled by the output signal of the voltage controlled oscillator. A 22K base resistor protects the base circuit and the relay coil resistance provides the load for the collector-emitter circuit. A 24 volt transistor power supply completes the relay control circuit. This relay is a standard ganged-action, double circuit model. The double circuit relay was used so that an indicating light could be incorporated in the system which would show whether the sampler relay was open or closed. The light is not necessary to the circuit except as a convenient visual aid in determining the position of the sampler relay or the approximate sampling rate. A GE-327 light was used.

The output of the voltage controlled, variable frequency oscillator is used to switch the transistor on and off. The



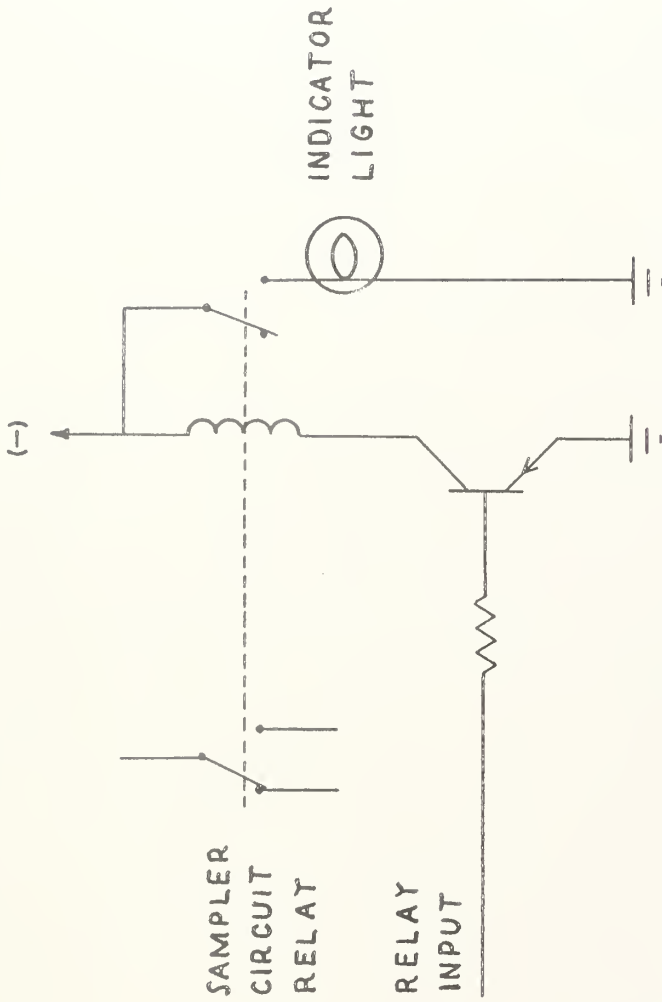


Figure E-1. Transistorized relay control circuit.



transistor operates in either non-conducting or saturated conducting states. The transistor acts as an on-off switch to open or close the 24 volt power supply which energizes the relay coil and thus opens or closes the relay in the sampler and zero order hold circuit. In this manner, the  $|\dot{E}|$  controlled, time variable frequency output of the voltage controlled oscillator determines the sampling frequency of the sampler and zero order hold.





## APPENDIX F

### Z-PLANE ROOT-LOCUS ANALYSIS

The root-locus analysis in the z-plane will provide a graphical method for observing the movement of the closed loop roots as a result of varying the sampling period or the open loop poles, zeros, or gain. The discussion will include one section for the analysis of a type I second order servo and one section for the analysis of a type II second order servo system.

#### Type I Servo

Given that  $G(s) = \frac{K}{s(s + b)}$  and the fixed period sampler is followed by a zero order hold as shown in Fig. F-1, then

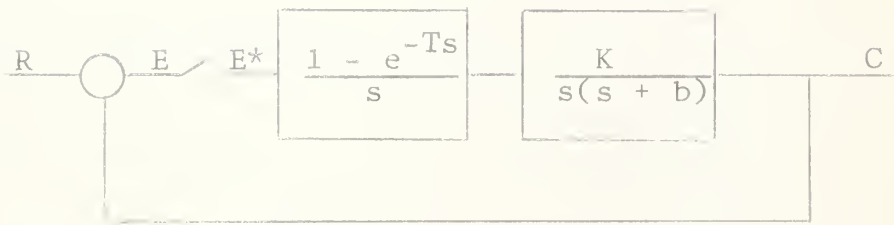


Fig. F-1. Sampled-data feedback control system.

the z transform  $G(z)$  is:

$$G(z) = \frac{K_1(z + z_1)}{(z - 1)(z - p_1)}$$

$$K_1 = \frac{K}{2} (bT + e^{-bT} - 1)$$

$$z_1 = \frac{1 - e^{-bT}(1 + bT)}{bT + e^{-bT} - 1}$$

$$p_1 = e^{-bT}$$

It is noted that, in general, the substitutions of the



functions of  $b$ ,  $K$ , and  $T$  for  $z_1$ ,  $p_1$ , and  $K_1$  will result in unwieldy expressions.

The limits on  $K_1$ ,  $z_1$ , and  $p_1$  are, for all values of  $K$ ,  $b$ ,  $T$  from zero to  $+\infty$  :

$$0 \leq K_1 \leq \infty$$

$$0 \leq z_1 \leq 1$$

$$0 \leq p_1 \leq 1$$

so the open loop zero  $z_1$  is always between  $z = 0$  and  $z = -1$  and the open loop pole  $p_1$  is always between  $z = 0$  and  $z = 1$ . The  $z$ -plane root-locus diagrams are shown in Table F-1.

By observing that the root-locus equation is:

$$\frac{K_1(z + z_1)}{(z - 1)(z - p_1)} = -1 \quad ,$$

where  $z = x + jy$  , then

$$\frac{K_1(x + z_1 + jy)}{(x - 1 + jy)(x - p_1 + jy)} = -1 \quad .$$

Solving the gain or phase equation shows that the curved portion of the root-locus is a circle with its center at  $-z_1$  and with radius

$$R = \left[ (z_1 + 1)(z_1 + p_1) \right]^{1/2} \quad .$$

The intercepts of the circle with the real axis are the root-locus breakaway points which are:

$$z = -z_1 \pm \left[ (z_1 + 1)(z_1 + p_1) \right]^{1/2} \quad .$$



SUMMARY OF Z-PLANE ROOT-LOCUS DIAGRAMS

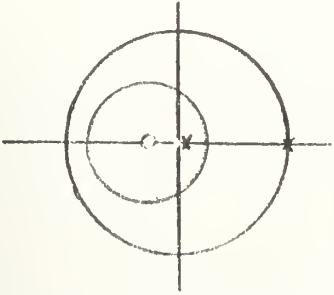
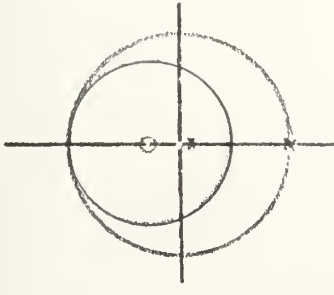
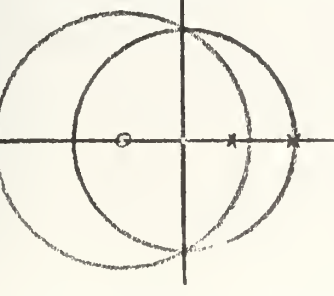
Root-locus configuration	Conditions for configuration	Gain range for stable response
 <p>all circular loci inside unit circle</p>	$z_1 < \frac{1 - p_1}{3 + p_1}$ $bT > 3.71$	$K_1 \leq \frac{2(1 + p_1)}{(1 - z_1)}$ $K \leq \frac{2b^2(1 + e^{-bT})}{bT(1 + e^{-bT}) - 2(1 - e^{-bT})}$
 <p>circular locus tangent to unit circle at <math>z = -1</math></p>	$z_1 = \frac{1 - p_1}{3 + p_1}$ $bT = 3.71$	$K_1 \leq 3 + p_1$ $K \leq \frac{b^2(3 + e^{-bT})}{(bT + e^{-bT} - 1)}$
 <p>all circular loci intersect the unit circle</p>	$z_1 > \frac{1 - p_1}{3 + p_1}$ $bT < 3.71$	$K_1 \leq \frac{1 - p_1}{z_1}$ $K \leq \frac{b^2(1 - e^{-bT})}{1 - e^{-bT}(1 + bT)}$

Table F-1. Summary of z-plane root-locus diagrams.



The double real roots occur at the two breakaway points and the gain at these points is:

$$K_1 = \frac{1}{R}(1+z_1+R)(z_1+p_1+R) = (2z_1+p_1+1) \pm \left[ (z_1+1)(z_1+p_1) \right]^{1/2}$$

Next, the critical value of  $z_{1c}$  is found such that the three root-locus configurations as listed in Table F-1 may be defined. The required relation is:

$$1 - z_{1c} = R = \left[ (z_{1c} + 1)(z_{1c} + p_1) \right]^{1/2},$$

and the solution is:

$$z_{1c} = \frac{1 - p_1}{3 + p_1},$$

and in terms of  $b$  and  $T$ :

$$z_{1c} = \frac{1 - e^{-bT}}{3 + e^{-bT}}.$$

The maximum gain for stability will now be determined for each of the three configurations. For  $bT < 3.71$  the maximum gain for stability is determined by the intersection of the root-locus circle and the unit circle. Three equations result; namely,

$$x^2 + y^2 = 1$$

$$(z_1 + x)^2 + y^2 = R^2 = (z_1 + 1)(z_1 + p_1)$$

$$K_{1m}^2 = \frac{\left[ (1 - x)^2 + y^2 \right] \left[ (x - p_1)^2 + y^2 \right]}{(z_1 + 1)(z_1 + p_1)}$$





These equations reduce to:

$$K_{1m} = \frac{1 - p_1}{z_1} \quad (bT < 3.71)$$

and in terms of  $b$  and  $T$  :

$$K = \frac{b^2(1 - e^{-bT})}{1 - e^{-bT}(1 + bT)} \quad (bT < 3.71)$$

for the maximum gain for stable response. Similarly,

$$K_{1m} = \frac{2(1 + p_1)}{(1 - z_1)} \quad (bT > 3.71)$$

$$K = \frac{2b^2(1 + e^{-bT})}{bT(1 + e^{-bT}) - 2(1 - e^{-bT})} \quad (bT > 3.71)$$

for the maximum gain for stable response. For the final configuration:

$$K_{1m} = 3 + p_1 \quad (bT = 3.71)$$

$$K = \frac{b^2(3 + e^{-bT})}{(bT + e^{-bT} - 1)} \quad (bT = 3.71)$$

for the maximum gain for stable response. A summary of these results is compiled in Table F-1.

It is to be noted that for a fixed value of  $b$  and a fixed value of  $T$ , variable values of the open loop gain  $K$  will then move the closed loop roots on the same fixed root-locus circle (assuming  $K$  produces roots in the circular locus range) since the values of  $p_1$  and  $z_1$  are unchanged. For fixed  $b$  and fixed  $K$  values, variable values of  $T$  will cause the values of  $p_1$ ,  $z_1$ , and  $K_1$  to be changed so the



closed loop roots will be moved to a different root-locus circle because of the new  $p_1$  and  $z_1$  values, and the roots will probably be moved to a different position on the new root-locus circle because of the new  $K_1$  value. For fixed  $K$  and  $T$  values, variable values of  $b$  will cause the values of  $p_1$ ,  $z_1$ , and  $K_1$  to be changed so the closed loop roots will be moved to a different root-locus circle because of the new  $p_1$  and  $z_1$  values, and the roots will probably be moved to a different position on the new root-locus circle because of the new  $K_1$  value.

Also note that if  $b$  is changed to the new value  $c_1 b$  (where  $c_1$  is a positive real constant) and  $T$  is changed to the new value  $T/c_1$  so that the product  $bT = (c_1 b)(T/c_1) = bT$  is unchanged, then the closed loop root positions will be moved on the same fixed root-locus circle since the root-locus gain  $K_1$  has been changed by the factor  $1/c_1^2$  even though  $z_1$  and  $p_1$  are unchanged in value.

### Type II Servo

Given that  $G(s) = \frac{K(s + a)}{s^2}$ , and the fixed period

sampler is followed by a zero order hold as in the system of Fig. F-1, then the  $z$  transform  $G(z)$  is:

$$G(z) = \frac{K_1(z + z_1)}{(z - 1)^2} \qquad \begin{aligned} K_1 &= KT(1 + \frac{aT}{2}) \\ z_1 &= \frac{aT - 2}{aT + 2} \end{aligned}$$



The unrestricted limits on  $K_1$  and  $z_1$  are, for all values of  $K, a, T$  from zero to  $+\infty$  :

$$0 \leq K_1 \leq \infty$$

$$-1 \leq z_1 \leq 1 .$$

The root-locus equation is:

$$\frac{K_1(z + z_1)}{(z - 1)^2} = -1 .$$

Substituting  $z = x + jy$ , and reducing the resulting equation gives:

$$(z_1 + 1)^2 = (x + z_1)^2 + y^2 .$$

The resulting equation is the equation of a circle with center at  $z = -z_1$ , radius  $R = z_1 + 1$ , and always contains the point  $z = 1$ . The root-locus diagram is illustrated in Fig. F-2.

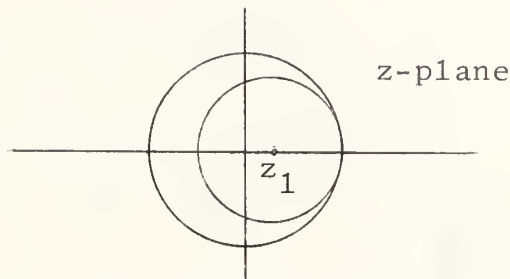


Fig. F-2. Root-locus diagram where  $-1 \leq z_1 \leq 0$

As in the case of the type I system, there are again three root-locus configurations; namely, (1) the root-locus circle inside the unit circle and tangent at  $z = 1$ , (2) the root-locus circle coincident with the unit circle, and (3) the



root-locus circle outside the unit circle and tangent at  $z = 1$ . Of course, the system response is always unstable for configuration (3) and always conditionally stable for configuration (2) and, therefore, these two configurations will not be considered. In order to obtain configuration (1), the open loop zero must be in the range  $-1 \leq z_1 \leq 0$  and only in this range. Because of the range of  $z_1$ , any expression involving  $(+z_1)$  can be rewritten with  $(-|z_1|)$ ; e.g., the radius of the root-locus circle is  $R = 1 + z_1 = 1 - |z_1|$  and the center of the root-locus circle is at  $z = -z_1 = |z_1|$ .

The circular root-locus portion has gain range  $0 \leq K_1 \leq 4R$ , which is:

$$0 \leq K_1 \leq 4(1 + z_1) .$$

The gain for the entire stable response region is:

$$0 \leq K_1 \leq \frac{(2)(2)}{1 - z_1} .$$

In terms of  $a$ ,  $K$ , and  $T$ , this range becomes:

$$0 \leq KT\left(1 + \frac{aT}{2}\right) \leq \frac{4}{1 - \frac{aT - 2}{aT + 2}} ,$$

which reduces to:

$$0 \leq KT \leq 2 .$$

Also, since  $-1 \leq z_1 \leq 0$ , then  $-1 \leq \frac{aT - 2}{aT + 2} \leq 0$ ,

which becomes:  $0 \leq aT \leq 2$ .

Thus, there are simultaneous conditions on  $T$ ; namely,

$$0 \leq aT \leq 2$$

and  $0 \leq KT \leq 2$ ,





which conveniently separate so that:

$$0 \leq T \leq \frac{2}{a} \quad (\text{for } a > K)$$

and 
$$0 \leq T \leq \frac{2}{K} \quad (\text{for } a < K)$$

are the conditions on  $T$  in order to have a stable response. Notice that these expressions for the range of  $T$  for stability are simple and straightforward compared to the same expressions for the type I system.

The closed loop root positions of the type II system are repositioned in the same manner as are the type I system roots with respect to varying one of the fixed values  $K$ ,  $a$ , or  $T$ , while holding the other two values fixed.













thesF233

Adaptive sampling frequency for sampled-



3 2768 002 13386 0  
DUDLEY KNOX LIBRARY